The type VI secretion system governs strain maintenance in a wild mammalian gut microbiome

Beth A. Shen[1], Kyle L. Asfahl[2], Bentley Lim[3], Savannah K. Bertolli[1], Samuel S. Minot[4], Matthew C. Radey[1], Kelsi Penewit[5], Billy Ngo[1], Stephen J. Salipante[5], Christopher D. Johnston[6], S. Brook Peterson[1,8], Andrew L. Goodman[3], and Joseph D. Mougous[1,2,7,8*]

[1]Department of Microbiology, University of Washington, Seattle, WA, USA
[2]Microbial Interactions & Microbiome Center, University of Washington, Seattle, WA, USA
[3]Department of Microbial Pathogenesis and Microbial Sciences Institute, Yale University School of Medicine, New Haven, CT, USA
[4]Bioinformatics Core, Fred Hutchinson Cancer Center, Seattle, WA, USA
[5]Department of Laboratory Medicine and Pathology, University of Washington, Seattle, Washington, United States of America.
[6]Department of Genomic Medicine, The University of Texas MD Anderson Cancer Center Houston, Houston, TX, USA
[7]Howard Hughes Medical Institute, University of Washington, Seattle, WA, USA
[8]Current address: Department of Microbial Pathogenesis and Microbial Sciences Institute, Yale University School of Medicine, New Haven, CT, USA

* To whom correspondence should be addressed:

Email – joseph.mougous@yale.edu

Abstract

Bacteria inhabiting the mammalian gut coexist in dense communities where contact-dependent antagonism mechanisms are widespread. The type VI secretion system (T6SS) is an interbacterial toxin delivery pathway prevalent among gut Bacteroidales, yet its function in naturally evolved microbiomes remains poorly defined. Here, we examine the physiological role of the T6SS in *Bacteroides* within a gut community derived from wild mice (the WildR microbiome). Using newly developed genetic tools and a strategy for functional replacement of strains within the WildR community, we demonstrate that the WildR isolate *B. acidifaciens* employs a T6SS to antagonize co-resident Bacteroidales. We also show that loss of T6SS function compromises the long-term maintenance of *B. acidifaciens* in the community but not its initial colonization, establishing the system as a determinant of strain persistence. The T6SS we identified resides on an integrative and conjugative element (ICE). ICE-seq, a targeted sequencing approach, reveals that the T6SS-ICE is distributed among select *Bacteroidales* and *Muribaculaceae* species in the WildR microbiome, between which it appears to be recently exchanged. We also show that transfer of the T6SS-ICE to WildR isolate *Phocaeicola vulgatus* confers transient colonization benefits in mice, but an eventual fitness cost. Our findings demonstrate that the T6SS can stabilize the presence of specific strains within a complex, co-evolved gut microbiome, yet its value is context dependent and constrained by the ecological and physiological landscape of the host community.

48 **Introduction**

49 Pathways for contact-dependent antagonism between bacteria are prevalent among
50 species residing in the densely colonized mammalian gut (Coyne et al. 2016, Verster et al. 2017,
51 Whitney et al. 2017, Garcia-Bayona and Comstock 2018). Prominent among these is the
52 bacterial type VI secretion system (T6SS), a mechanism employed by Gram-negative species to
53 deliver toxic effector proteins directly to contacting Gram-negative cells (Hood et al. 2010,
54 Schwarz et al. 2010, Coulthurst 2019). The T6SS is widely distributed among gut resident
55 species belonging to the Bacteroidota phylum. Over half of *Bacteroides* spp. isolated from
56 mammalian gut samples encode T6SS genes, and Bacteroidales T6SS effector genes can be
57 found in >60% of individual human metagenomic datasets (Verster et al. 2017, Garcia-Bayona et
58 al. 2021). *In vitro* experiments suggest the T6SS of *Bacteroides* spp. can target a broad cross
59 section of gut Bacteroidales, while it does not appear to act on Proteobacteria, the second most
60 abundant group of Gram-negative organisms in the gut (Chatzidaki-Livanis et al. 2016).

61 A number of model murine gut microbiome studies have sought to provide insight to the
62 role of the Bacteriodales T6SS in the gut. Studies employing gnotobiotic animals co-colonized
63 by pairs of strains demonstrate that T6SS-mediated killing can occur in this environment, and
64 show that targeting in laboratory co-cultures is not necessarily diagnostic of an interaction
65 between strains in the murine intestine(Chatzidaki-Livanis et al. 2016, Wexler et al. 2016, Ross
66 et al. 2019, Robitaille et al. 2023, Sheahan et al. 2024). Gnotobiotic experiments in which more
67 complex mixtures of bacteria (up to 12 species) are co-inoculated and colonization of
68 conventional mice with pairs of *Bacteroides* strains demonstrate T6SS-mediated antagonism can
69 occur in the context of a more diverse assemblage (Hecht et al. 2016, Wexler et al. 2016, Hill et
70 al. 2024). However, these experiments all suffer from a number of limitations. For instance, the

71 species employed are not native to the mouse gut, and the antagonistic interactions being
72 assessed are between strains that may have never co-inhabited a natural community. Gnotobiotic
73 experiments additionally suffer from the lack of community complexity, while experiments
74 employing conventional animals require antibiotic pre-treatment or large inoculums to enable
75 strain engraftment (Hecht et al. 2016, Hill et al. 2024). As a result of these limitations, the
76 physiological role of the T6SS in mammalian gut microbial communities remains largely
77 unknown.

78 The limited insights available into the function of the T6SS in native gut microbiomes
79 primarily derive from metagenomic analyses of T6SS gene distribution patterns. T6SS gene
80 clusters in Bacteroidales segregate into three Genetic Architectures (GA) 1-3 based on synteny
81 and evolutionary relatedness; however, each contain conserved structural genes and variable
82 effector and cognate immunity genes (Coyne et al. 2016). GA1 and GA2 loci are encoded on
83 mobile elements, and several studies show they can be horizontally exchanged among
84 Bacteroidales strains co-resident in a microbiome, suggesting a selective benefit to obtaining
85 T6SS effector and immunity genes shared by neighboring species (Coyne et al. 2014, Garcia-
86 Bayona et al. 2021, Sheahan et al. 2024). Further evidence supporting selection for compatibility
87 among the T6SS effector repertoire in co-resident species lies in the finding that effector gene
88 diversity in individual microbiomes is low, in contrast to the high degree of effector diversity
89 observed across metagenomes (Verster et al. 2017). Studies have also revealed that gut
90 Bacteroidales species can encode clusters of T6SS immunity genes unlinked to cognate effectors
91 (Ross et al. 2019). One type of these acquired interbacterial defense (AID) gene clusters,
92 designated rAID for recombinase-associated, are widely distributed across Bacteroidales and
93 have features consistent with active acquisition of additional immunity genes. A subset of genes

encoded within AID and rAID systems selectively neutralize T6SS toxins, indicative of the selective benefit of resisting T6SS-based intoxication in the gut environment. However, other evidence suggests that under certain conditions the cost of producing a T6SS can outweigh its benefit. Studies of the prevalence of T6SS genes among *B. fragilis* strains reveal they are more common in the microbiomes of infants than in adults (Verster et al. 2017, Robitaille et al. 2023). Furthermore, longitudinal sampling of individual human gut microbiomes has revealed instances in which the *B. fragilis* T6SS acquires inactivating mutations over time(Robitaille et al. 2023). A comprehensive understanding of the physiological role of the T6SS in gut *Bacteroidales* has thus yet to emerge.

Experimental testing of the hypotheses regarding T6SS function generated from metagenomic and theoretical studies requires a tractable experimental model substantially more representative of natural gut communities than those that have been employed to date. Here, we study the function of a Bacteroidales T6SS in a natural gut community derived from wild mice and reintroduced into gnotobiotic animals (Rosshart et al. 2017). We show that this community retains a similar composition and level of diversity as the wild mouse community from which it derives, and we demonstrate we can functionally replace members of the community by adding an excess of a mutant strain of interest at the time of community introduction. Using this approach, we demonstrate that the T6SS of *B. acidifaciens* is important for maintaining this species in the community. We also demonstrate T6SS-mediated targeting between *Bacteroides* species from the same gut microbiome, and provide evidence that not all Bacteroidales in the community benefit from horizontal acquisition of the T6SS. Together, our findings show that the T6SS can be an important fitness determinant in a native gut community of naturally co-occuring organisms, and that its contribution to competitiveness in the gut varies across species.

117

118 **Results**

119 **The WildR microbiome is stable and similar to wild mice microbiomes despite propagation**

120 The WildR microbial community consists of a complex assemblage of organisms
121 obtained from the pooled ileocecal contents of three wild mice and subsequently introduced to
122 germ-free mice for laboratory propagation (Rosshart et al. 2017). This community diverges
123 substantially from that found in lab-reared mice, with a significantly greater proportion of strains
124 from the Bacteroidota and Pseudomonodata phyla, and a lower proportion of Bacillota and
125 Verrucomicrobia. Additionally, the most abundant OTUs in the WildR population are
126 consistently missing from lab mouse microbiomes. Importantly, by the F4 generation of
127 laboratory propagation in mice, much of the diversity of the WildR was retained, and its
128 composition was indistinguishable from that found in the originally gavaged dams (Rosshart et
129 al. 2017).

130 To establish whether mice colonized by the WildR community could serve as an
131 appropriate model to study T6SS-mediated interactions in the gut, we first sought to determine
132 whether community composition diverged in the subsequent generations of propagation since its
133 initial study. We obtained ileocecal contents of the F7 WildR generation, introduced these to
134 gnotobiotic mice via oral gavage, then harvested and cryopreserved cecal contents after 14 days
135 of *in vivo* propagation of the community (Supplemental Figure 1A). To assess the phylogenetic
136 composition of the WildR microbiome after this propagation, we performed short-read
137 metagenomic sequencing on DNA extracted from two stored aliquots and two fecal pellets from
138 mice used to propagate the community, generating a total of 63 Gb of sequence data. Reads were
139 then mapped to a mouse microbiome-specific reference database using Kraken 2 (Wood et al.

140 2019). This analysis revealed that, like the initial wild mouse microbiome samples and F2
141 generation, the WildR F7 community is enriched for Bacteroidota and depleted in Bacillota
142 compared to that of lab reared mice (Figure 1A, Supplemental Table 1). Comparison of the
143 relative abundance of the 100 most prevalent genera in the wild donor mice across each
144 community indicated strong correlations between the wild, WildR F2 and Wild F7 communities
145 (Figure 1B, C, Supplemental Figure 1B). In contrast, lab mouse microbiomes diverge
146 substantially from these communities, and lack 24 genera found in each wild-mouse derived
147 microbiome (Figure 1D, E, Supplemental Figure 1C).
148
149 **Two WildR species share a mobile T6SS**
150 Having determined that the overall community composition and diversity found in wild
151 mouse microbiomes is preserved in the WildR F7 generation, we aimed to identify organisms in
152 the community that encode T6SS genes. Toward this end, we used metagenomic and long-read
153 sequencing data from WildR F7 samples to assemble high quality metagenome associated
154 genomes (MAGs). In parallel, we obtained genome sequences for 15 strains isolated from the
155 community. In total, we generated nine closed and six draft genomes from isolates and 72 MAGs
156 with an average contig N50 of 946 kb (Supplemental Table 2). Collectively, these genomes
157 represent ~50% of the species level diversity present in the community (Supplemental Figure
158 1D).
159 Within our collection of WildR-derived genomes, we identified three encoding T6SS
160 genes. These include genomes from isolates of *B. acidfaciens* and *B. caecimuris* and a MAG
161 identified as deriving from *Mucispirillum schaedleri.* The latter species is a member of the
162 Chrysiogenota phylum (formerly Deferribacteres) for which no genetic tools are available. Thus,

163 with the aim to functionally investigate the role of the T6SS using the WildR model, we focused
164 on the more tractable *Bacteroides* spp. systems. We found that the T6SSs present in the WildR
165 *B. acidfaciens* and *B. caecimuris* strains we isolated exhibit the GA1 architecture and are nearly
166 identical across the gene cluster (Figure 1F). Like GA1 systems identified in other species, the
167 T6SS appears to be encoded on an integrative and conjugative element (ICE) (Coyne et al.
168 2016). The ICE encompasses a 115 kb region, includes genes coding for DNA transfer and
169 assorted other functions, and is identical between the genomes except for a one base-pair
170 deletion within a predicted effector of the *B. caecimuris* GA1 cluster (Supplemental Figure 1E).
171 This degree of similarity is consistent with recent exchange of the element between the species;
172 previous studies of human microbiome isolates found that GA1 elements from strains co-resident
173 in the same individual share >99% sequence identity, while those of strains isolated from
174 different individuals share 95-98% identity(Coyne et al. 2016, Garcia-Bayona et al. 2021).
175 Interestingly, the T6SS we found in *B. acidifaciens* and *B. caecimuris* shares only 82-83%
176 identity with previously identified GA1 systems found in human isolates, suggesting the ICE is
177 not being frequently exchanged between human and murine-adapted *Bacteroides* species
178 (Supplemental Table 3).
179 Within the *B. acidfaciens* and *B. caecimuris* T6SS loci, we identified two candidate
180 secreted effector genes (BA_01695 and BA_01705 in *B. acidifaciens*; Figure 1F, G). The
181 predicted toxins contain N-terminal PAAR and Rhs domains, which are common among T6SS
182 effectors. The C-terminal toxin domains of these proteins share no significant sequence
183 homology or predicted structural similarity with characterized proteins. However, conserved
184 domain analysis and comparison to structural models in the AlphaFold database indicated that
185 both bear features of predicted nuclease toxins. BA_01695, herein renamed Bae1 (*B.*

186 *acidifaciens* effector 1), contains the AHH predicted nuclease domain, while the toxin domain of
187 BA_01705, renamed Bae2, resembles the enzymatic domain of endonucleases in the GIY-YIG
188 family. Genes conferring immunity to T6SS system toxins are typically small open reading
189 frames (ORFs) encoded immediately downstream of their cognate effector. Indeed, we found a
190 putative immunity gene downstream of *bae1* (BA_01696, renamed *bai1*); a candidate immunity
191 gene for Bae2 is located just upstream of the toxin gene (BA_01704, renamed *bai2*), and encodes
192 a protein domain previously classified as an immunity determinant (Figure 1G). Interestingly, the
193 single base-pair difference between the T6SSs of *B. acidifaciens* and *B. caecimuris* occurs within
194 the *bae1* gene of *B. caecimuris*, introducing a likely inactivating frameshift (Supplemental Figure
195 1E). Therefore, we focused our initial functional studies of the T6SS in the WildR community on
196 *B. acidifaciens.*
197
198 **The *B. acidifaciens* T6SS intoxicates WildR Bacteroidales**
199 As a first step toward understanding the role played by the *B. acidifaciens* T6SS in
200 WildR-colonized mice, we sought to determine which, if any, members of the community are
201 susceptible to intoxication by this system *in vitro*. However, these efforts were initially
202 confounded by our inability to genetically manipulate the WildR *B. acidifaciens* isolate using
203 previously published approaches (Garcia-Bayona and Comstock 2019, Bencivenga-Barry et al.
204 2020). We hypothesized that, as in other wild isolates, restriction modification (RM) systems
205 constitute a significant barrier to the introduction of foreign DNA in this strain (Johnston et al.
206 2019). To circumvent this problem, we applied the previously described RM-silencing
207 SyngenicDNA approach (Johnston et al. 2019). Using single-molecule sequencing, we identified
208 eight distinct methylated motifs in *B. acidifaciens* (Supplemental Table 4), representing a

209 complex RM system barrier within this strain. Elimination of the single methylated motif found
210 in the integrative plasmid pNUB2 enabled us to obtain transconjugants with the plasmid
211 harboring a *B. acidifaciens* gene of interest (*tssC*), which was otherwise recalcitrant to transfer
212 (Supplemental Figure 2A). Although conjugation is often considered relatively insensitive to RM
213 barriers, these data indicate that the RM landscape can substantially limit conjugative plasmid
214 transfer in wild Bacteroides (Dimitriu et al. 2024). Thus, we applied this same RM silencing
215 approach to generate a series of improved plasmids for allelic exchange, which were used to
216 successfully inactivate several T6SS effector, immunity and structural genes from *B.*
217 *acidifaciens.*

218 To confirm that Bae1 and Bae2 are active T6SS effectors, we performed *in vitro* growth
219 competition assays under contact-promoting conditions using wild-type *B. acidifaciens* and
220 mutants sensitized to one or both of the toxins by deletion of the predicted immunity
221 determinants. These experiments revealed that co-cultivation with the wild-type strain inhibits
222 the growth of mutants sensitized to Bae1 or Bae2 through immunity gene inactivation (Figure
223 2A). A strain lacking a functional T6SS (*B. acidifaciens* Δ*tssC*) did not inhibit the effector-
224 sensitized strains, indicating both Bae1 and Bae2 are delivered via the T6SS and have the
225 capacity to inhibit target cell growth. We then used similar assays to measure T6SS targeting of
226 other strains isolated from the WildR community. Like the T6SS of other Bacteroidales, we
227 found that targets of the *B. acidifaciens* system were restricted to members of the same order
228 (Figure 2B)(Russell et al. 2014, Chatzidaki-Livanis et al. 2016, Wexler et al. 2016). Given that
229 the fitness benefit conferred by the T6SS in these experiments was relatively modest (<10 fold),
230 we also generated two additional T6SS inactivated mutants of *B. acidifaciens* (Δ*clpV* and Δ*tssN*).
231 These strains exhibited a similar competitive defect against *B. caeicimuris* F5 and *Phocaeicola*

232 *vulgatus* as *B. acidifaciens* Δ*tssC*, and the phenotype could be complemented by heterologous
233 expression of the inactivated genes (Supplemental Figure 2B, C). There were also Bacteroidales
234 for which we were unable to observe evidence of targeting by the *B. acidifaciens* T6SS. As
235 expected, the *B. caecimuris* strain F12, which carries homologs of *bai1* and *bai2* within its T6SS
236 gene cluster, is resistant to targeting. With the exception of *B. uniformis*, the other strains
237 resistant to target are Bacteroidales from outside of the genus *Bacteroides*. Importantly,
238 examination of the metagenomic data from two of the wild mice used to generate the WildR
239 revealed that *B. acidifaciens*, and each of the candidate target species we tested were detected in
240 both animals, indicating the interaction patterns we observe are reflective of T6SS targeting
241 between species co-resident within a natural microbiome (Figure 2C). Together, these results
242 demonstrate the potential for T6SS-mediated targeting between members of the same natural gut
243 community.

244 Previous studies indicate that the range of T6SS-mediated targeting observed for
245 Bacteroides strains during *in vitro* growth assays does not necessarily predict *in vivo* interactions
246 (Wexler et al. 2016). Thus, we used co-colonization of gnotobiotic mice assays to evaluate the *B.*
247 *acidifaciens* T6SS targeting capacity in the murine gut. As a first test of T6SS activity in this
248 environment, we assessed the ability of *B. acidifaciens* wild-type or Δ*tssC* to intoxicate an
249 immunity-deficient target strains (Δ*bae1*Δ*bai1*Δ*bae2*Δ*bai2*). By 14 days after introduction of the
250 strain pairs by co-gavage, we found the immunity-deficient strain was significantly depleted in
251 the presence of wild-type but not T6SS-inactive *B. acidifaciens,* and decline of the immunity-
252 deficient population continued until the end of the experiment 35 days post-gavage (Figure 2D).
253 We then used this model to evaluate *B. acidifaciens* T6SS-mediated targeting of two strains we
254 found to be susceptible to intoxication by the system *in vitro, B. caecimuris* F5 and *P. vulgatus.*

255 During co-colonization with wild-type *B. acidifaciens, in vivo* growth of *B. caecimuris* F5 was
256 largely inhibited, whereas by 28 days post gavage with *B. acidifaciens* Δ*tssC*, this strain became
257 the predominant population in fecal samples (Figure 2E, Supplemental Figure 2D). To our
258 knowledge, these data represent the first demonstration of *in vivo* T6SS-mediated targeting
259 between *Bacteroidales* strains derived from the same natural gut microbiome.
260 In contrast to the dynamics observed during *B. acidifaciens–B. caecimuris* co-
261 colonization experiments, we found that T6SS inactivation had little impact when *B. acidifaciens*
262 was introduced to gnotobiotic mice along with *P. vulgatus* (Supplemental Figure 2E, F). In these
263 experiments, *P. vulgatus* quickly became the predominant colonizer regardless of the T6SS
264 activity of *B. acidifaciens*, representing ~80% of the total population by 7 days post gavage. This
265 overall level of competitiveness of *P. vulgatus* is consistent with the predominance of this
266 species among Bacteroidales in the WildR community (Supplemental Figure 2G).
267
268 **A method for modified strain introduction into the WildR**
269 Evaluating the role of the *B. acidifaciens* T6SS in the context of WildR colonized mice,
270 requires a method to introduce mutant strains into the community. Prior studies of strain
271 engraftment indicate that priority effects and competitive exclusion are barriers to introducing a
272 derivative strain to an established microbiome containing the parent or closely related strains
273 (Lee et al. 2013, Maldonado-Gomez et al. 2016, Obadia et al. 2017, Martinez et al. 2018, Segura
274 Munoz et al. 2022). Additionally, previously proposed methods for manipulating microbiomes *in*
275 *situ* with antibiotic treatments followed by delivery of a new strain or *in situ* genetic engineering
276 suffer from the requirement to identify antibiotics or *in vivo* amenable genetic tools that
277 specifically target a species of interest (Jin et al. 2022, Rubin et al. 2022, Segura Munoz et al.

278 2022). Given that our method of introducing the WildR community to the murine gut involves
279 oral gavage of the mixed population and its subsequent establishment, we hypothesized that we
280 could circumvent these challenges and facilitate colonization of *in vitro* modified *B. acidifaciens*
281 isolate by taking advantage of the natural carrying capacity of the gut microbiome (Lee et al.
282 2013, Hecht et al. 2016, Segura Munoz et al. 2022). Specifically, we reasoned that the addition
283 of an excess of a *B. acidifaciens* modified strain to the WildR community during gavage would
284 lead to displacement of the endogenous *B. acidifaciens* population while maintaining the overall
285 natural composition of the WildR community (Figure 3A).

286 To test this hypothesis, we assessed the potential for *B. acidifaciens* marked with
287 erythromycin resistance (*B. acid* ^{exo}) to replace the endogenous population (*B. acid* ^{endo}) when
288 titrated into the WildR gavage mixture at different levels (Figure 3A). In cryopreserved samples
289 of the F7 WildR community, we determined that *B. acid* ^{endo} is present at ~$3x10^4$ CFU/mL (see
290 Methods). We then added 1x, 10x, or 100x *B. acid* ^{exo} relative to this population ($3x10^4$-$3x10^6$
291 CFU/mL) to aliquots of the reference stocked WildR community and inoculated mice via oral
292 gavage. Supporting our hypothesis that endogenous *B. acidifaciens* populations represent the
293 carrying capacity for this species in the murine gut microbiome, we found that addition of 100-
294 fold excess *B. acidifaciens* in the gavage did not significantly increase the total relative
295 abundance of the species in mice at 7 days post-gavage (Figure 3B). We also observed that at
296 each titration level, we successfully replaced ~80% of the *B. acid* ^{endo} population with the marked
297 strain; this frequency is likely an underestimate due to the detection limit of the qPCR-based
298 method used for distinguishing the strains (Figure 3C). Higher titrations of the marked strain
299 resulted in a trend toward lengthening its persistence in the community, although this effect was
300 not statistically significant (Figure 3D, Supplemental Figure 3A, B). Additionally, β-diversity

301 analyses of 16S rRNA amplicon sequences revealed that *B. acid* ^{exo} addition did not impact
302 overall community composition, regardless of the inoculum level employed (linear mixed effects
303 model P>|z| > 0.05 for all comparisons, Figure 3E).
304
305 **Long-term maintenance of *B. acidifaciens* in the WildR community requires the T6SS**
306 With a method in hand for introducing a genetically modified strain into the WildR
307 community, we applied this approach toward dissecting the physiological role of the *B.*
308 *acidifaciens* T6SS. Our experiment was designed to test two different possible roles that have
309 been proposed for the T6SS of *Bacteroides* in the gut microbiome: *i*) facilitating niche
310 establishment during initial colonization and *ii*) population maintenance once stable colonization
311 is achieved (Hecht et al. 2016, Verster et al. 2017, Robitaille et al. 2023). Germ-free mice were
312 co-gavaged with either *B. acid* ^{exo} or *B. acid* ^{exo} Δ*tssC* and the WildR community. *B. acid* ^{exo}
313 populations in fecal samples were then monitored over time by plating on selective media, and
314 the proportion of the total *B. acidifaciens* population represented by *B. acid* ^{exo} was monitored by
315 qPCR. We found that through 14 days post gavage, population levels of *B. acid* ^{exo} and *B. acid* ^{exo}
316 Δ*tssC* were indistinguishable (Figure 3E, Supplemental Figure 3E). However, by day 28, *B. acid*
317 ^{exo} Δ*tssC* was significantly depleted from the community compared to the marked wild-type
318 parent strain. By 56 days post gavage, we observed a nearly 100-fold difference in the abundance
319 of the two strains in both fecal and cecal content samples (Figure 3F, Supplemental Figure 3F).
320 To confirm that inactivation of the T6SS is responsible for the depletion of *B. acid* ^{exo} Δ*tssC*, and
321 not a secondary site mutation, we sequenced the genomes of the strains employed in the
322 experiment. *B. acid* ^{exo} Δ*tssC* used in the first replicate of the experiment carried a single
323 synonymous mutation (in *cdr*) and in the second replicate the strain bore no mutations. Of note,

324 the marked wild-type *B. acid* ^{exo} population also declined over time relative to endogenous *B.*
325 *acidifaciens* levels, while the overall abundance of *B. acidifaciens* in the community remained
326 similar throughout the experiment (Figure 3G, H); we hypothesize that the decline of *B. acid* ^{exo}
327 derives from a fitness cost associated with carrying the erythromycin resistance marker.
328 However, this decline was modest compared to the decrease in abundance of *B. acid* ^{exo} Δ*tssC*.
329 To determine which organisms could be the targets of the *B. acidifaciens* T6SS, we
330 performed 16S rRNA amplicon sequencing on fecal samples from mice colonized by the two *B.*
331 *acid* ^{exo} strains and parallel control mice colonized with the WildR community alone. This
332 analysis revealed no significant differences between the three communities at any of the time
333 points sampled (Supplemental Figure 3G). One potential explanation for this finding is *B.*
334 *acidifaciens* is present at significantly lower abundance in the community than the organism(s) it
335 targets. In this scenario, T6SS-targeting could be required for *B. acidifaciens* population survival
336 without causing a sufficiently large decrease in the population of the target to be detectable by
337 the relatively low-resolution measurement method we employed. Consistent with this potential
338 explanation for the lack of overall community shift upon inactivation of the *B. acidifaciens*
339 T6SS, we find that this species is present at 5 to 10-fold lower abundance than five other
340 Bacteroidales species in WildR F7 samples (Supplemental Figure 2G). Together, our results
341 suggest that the T6SS is required for *B. acidifaciens* population maintenance in the gut, but
342 dispensable for initial colonization.
343
344 **Distribution of a mobile T6SS in the WildR community**
345 Given the fitness benefit of the T6SS we observed for *B. acidifaciens* during stable
346 colonization of the mouse gut, and previous observations that T6SS-containing ICE can be

347 present in multiple species in a single microbiome (Coyne et al. 2014, Zhang et al. 2024), we
348 sought to better understand the distribution of the system in the WildR community. To avoid
349 both the biases inherent in screening for the element in cultured isolates and the challenges of
350 assigning repetitive sequences from metagenomic datasets to MAGs, we developed a targeted
351 sequencing-based approach for identifying ICE-carrying strains in DNA extracted directly from
352 WildR-colonized mouse fecal samples. Our method, which we named ICE-seq, is based on
353 techniques used for identifying transposon insertion locations (Gallagher 2019). In short, we
354 designed primers to specifically amplify and sequence outward from the 5' and 3' ends of the
355 ICE to capture the genomic context of the insertion (e.g., ICE junctions; Supplemental Figure
356 4A). After amplification and sequencing of ICE junctions from fecal pellets collected from 4
357 WildR-colonized mice, reads were mapped to a large, dereplicated genome catalog containing
358 the WildR MAGs generated in this study and the comprehensive mouse microbiota genome
359 (CMMG) catalog to identify ICE-containing strains (Gallagher 2019, Kieser et al. 2022). We
360 assigned a positive identification of an ICE-containing strain based on the presence of reads
361 mapping from either end of the ICE that diverge from a single position on a contig.

362 Supporting the validity of our approach, we detected ICE insertion within *B. acidifaciens*
363 and *B. caecimuris* F12 (Figure 4A). For these and other species, detection of ICE and the
364 proportion of ICE-seq reads each represented varied between mice. For *B. acidifaciens* and *B.*
365 *caecimuris* F12, this appears to reflect their abundance in individual mice; however, we posit that
366 exchange of the ICE on a rapid timescale could explain the additional variability observed. We
367 also found three additional strains harboring the ICE: *Muribaculaceae* CAG-485 sp002362485,
368 *Bacteroides* spMGG23559, and *Phocaeicola sartorii*. In *Muribaculaceae* CAG-485
369 sp002362485, we identified four insertion locations for the ICE, suggesting there are multiple

370 populations of this species harboring the element within the community. To our knowledge,
371 T6SS-encoding ICE have not previously been detected in a Muribaculaceae family member.
372 Strikingly, we did not find evidence of ICE insertion in many of the more abundant
373 Bacteroidales species in the community, including *P. vulgatus, Bacteroides* sp. 910578895 and
374 *Parabacteriodes* sp. 910577325. These findings suggest that fitness benefits conferred by
375 acquiring the ICE could vary across species.
376
377 **Acquisition of a T6SS-encoding ICE transiently benefits *P. vulgatus***
378 Our finding that the ICE harboring a GA1 T6SS is shared by multiple Bacteroidales
379 species in the WildR community suggests that it can be exchanged among community members.
380 However, we also found that many WildR Bacteroidales species do not contain the element,
381 suggesting the fitness benefit is confers may be species-specific, or that barriers exist that
382 prevent its transmission to certain strains. To gain insight into the mechanisms governing ICE
383 distribution, we focused on *P. vulgatus,* a prominent member of the WildR community which
384 our ICE-seq analysis indicates does not naturally harbor the element (Figure 4A). Using *in vitro*
385 conjugation assays with *B. acidfaciens* in which we introduced a chloramphenicol resistance
386 cassette to the ICE, we were able to obtain integrants of the wild-type ICE and mutant
387 derivatives in *P. vulgatus* (Supplemental Figure 4B). Sequencing revealed the ICE inserts at
388 multiple locations in this strain characterized by a degenerate, AT-rich sequence (Supplemental
389 Figure 4C). These findings suggest that barriers to horizontal gene transfer are unlikely to
390 explain the lack of acquisition of the element by *P. vulgatus* in the context of the WildR.
391 Having obtained *P. vulgatus* strains carrying the ICE, we next asked whether the
392 transferred T6SS is functional in this context. Surprisingly, we found that *P. vulgatus* carrying

393 the element is able to use the ICE-encoded T6SS to robustly antagonize a range of Bacteroidales
394 strains isolated from the WildR, including the parent strain lacking the ICE (Figure 4B). We also
395 found that acquisition of the ICE by *P. vulgatus* enabled this strain to resist antagonism by *B.*
396 *acidifaciens* as a result of acquiring the immunity genes *bai1* and *bai2* (Figure 4C).
397 While our *in vitro* experiments suggest multiple potential fitness benefits for *P. vulgatus*
398 of acquiring the ICE, the fact that we fail to detect transfer of the element to this species in
399 WildR-colonized mice suggests it incurs a fitness cost under physiological conditions not
400 captured by our *in vitro* assays. To evaluate this possibility, we co-gavaged germ-free mice with
401 wild-type *P. vulgatus* and derivatives marked with an erythromycin resistance cassette integrated
402 at a neutral site and carrying the intact ICE, or a version of the ICE in which the T6SS is
403 inactivated (ICE Δ*tssC*). Strikingly, we found that despite their 10-fold excess in the gavage
404 sample, each ICE-containing strain was eventually supplanted by the wild-type parent (Figure
405 4D). Replacement occurred more rapidly when the T6SS on the ICE was inactivated, indicating
406 that T6SS mediated targeting of the parent strain likely occurred, but was insufficient to
407 compensate for the fitness cost incurred from acquisition of the element.
408 We next examined the fitness consequence to *P. vulgatus* of carrying the ICE in the
409 context of the WildR-colonized mouse intestine. Employing the same carrying capacity-
410 mediated approach for strain engraft we developed with *B. acidifaciens*, we colonized mice with
411 the WildR community and *P. vulgatus* strains carrying the wild-type or Δ*tssC* ICE (Figure 4E).
412 Up to three weeks post-gavage, *P. vulgatus* carrying the wild-type ICE colonized to higher levels
413 than *P. vulgatus* ICE Δ*tssC,* and dominated endogenous *P. vulgatus* populations (Figure 4F,
414 Supplemental Fig 4D). This result suggests that T6SS activity provides an advantage to *P.*
415 *vulgatus* early in the establishment of the gut community. However, by the conclusion of the

416 experiment, the abundance of *P. vulgatus* ICE declined significantly, with a concomitant rise in
417 endogenous *P. vulgatus* populations (Figure 4F, Supplemental Fig 4D). This contrasts with our
418 findings using germ-free mice co-colonized with endogenous *P. vulgatus* and *P. vulgatus* ICE, in
419 which we observed a cost to carrying the ICE at early time points (Figure 4D). We speculate that
420 in the context of the WildR, the competition from the increased diversity of species exerts greater
421 selection for antagonistic capacity. The extent of T6SS-mediated antagonism by *P. vulgatus*
422 carrying the ICE is supported by analysis of the overall community structure. In fecal samples
423 collected 14-21 days post gavage, when *P. vulgatus* ICE and ICE Δ*tssC* abundance differs, we
424 observe a significant degree of variation between the two communities (Supplemental Figure
425 4E). At later timepoints, the communities of mice colonized by the two strains were less distinct,
426 although they remained significantly divergent in one replicate.

427 The transient nature of the fitness benefit conferred to *P. vulgatus* by T6SS activity in
428 WildR-colonized mice contrasts with the long-term benefit to T6SS activity we observed for *B.*
429 *acidifaciens* (Fig 3E). Given that ICE acquisition by *P. vulgatus* would likely occur after
430 community establishment – a state in which our data suggest the element does not provide a
431 lasting benefit to *P. vulgatus* – these results offer an explanation for the lack of ICE in this
432 species. Interestingly, we found that while *P. vulgatus* ICE Δ*tssC* was initially less able to
433 colonize mice in the context of the WildR community than *P. vulgatus* carrying an active T6SS,
434 this strain persisted at similar population levels in a subset of mice throughout the duration of the
435 experiment (Figure 4F). This result was unexpected, given that *P. vulgatus* ICE Δ*tssC* was
436 rapidly displaced by the endogenous *P. vulgatus* strain in pairwise gnotobiotic mouse
437 colonization experiments (Figure 4D). This finding suggests that in the context of the WildR,
438 functions encoded on the ICE beyond toxin delivery by the T6SS provide a benefit to *P.*

439 *vulgatus*. Of note, *P. vulgatus* ICE Δ*tssC* carries the intact immunity genes and therefore retains
440 the capacity to resist intoxication by Bae1 and Bae2 (Figure 4C); these may contribute to the
441 fitness benefit of the element in the presence of the WildR, where these toxins could be delivered
442 by other T6SS-ICE encoding strains.
443
444 **Discussion**
445 In the stable mammalian gut microbiome, where individual strains can persist throughout
446 the lifetime of an individual, the role of interbacterial antagonism pathways is not well
447 understood. Modeling-based studies suggest that antagonistic relationships between community
448 members can be stabilizing to the community as a whole, but how these pathways are employed
449 in an established community and the degree to which active targeting occurs between community
450 members in this setting is unexplored (Coyte et al. 2015, Coyte and Rakoff-Nahoum 2019).
451 Here, we show that an active T6SS is required for persistence of the mouse commensal *B.*
452 *acidifaciens* in a natural murine gut community. To our knowledge, our results represent the first
453 evidence of T6SS-mediated targeting between naturally co-resident gut species. The species
454 targeted by the *B. acidifaciens* T6SS *in vivo* could not be confidently ascertained by the approach
455 we employed, likely because this strain represents a small fraction of the community and its
456 antagonistic activity did not detectably affect other populations. However, *in vitro* experiments
457 demonstrate that other Bacteroidales species from the same community are effectively targeted
458 by the T6SS of this organism. We postulate that *B. acidifaciens* relies on T6SS-mediated
459 antagonism to prevent displacement by competing *Bacteroides.* This model for the role of the
460 T6SS in gut Bacteroidales is consistent with metagenomic analyses showing that in adult human

461 gut microbiomes, *B. fragilis* is most likely to carry the T6SS if the overall prevalence of
462 *Bacteroides* species is high (Verster et al. 2017, Robitaille et al. 2023).
463 Under our experimental conditions, the T6SS of *B. acidifaciens* appears to be dispensable
464 for initial colonization of the murine gut. This result was unexpected, as the T6SS is more
465 prevalent in human infant gut microbiomes than in adults, suggesting that T6SS-mediated
466 competition between *Bacteroides* is important during microbiome establishment (Verster et al.
467 2017, Robitaille et al. 2023). The colonization dynamics associated with WildR introduction to
468 adult animals differ from the natural process of gut microbiome development. Modifications to
469 our carrying capacity-driven approach to strain engraftment will be needed to establish a model
470 that more faithfully replicates the early stages of natural gut microbiome establishment.
471 Additionally, our experiments did not address the role of the T6SS in resilience following
472 disturbance, nor in preventing strain invasion, both of which are questions that should be
473 amenable to future studies employing the WildR model.
474 A feature shared by the widely distributed GA1 and GA2 T6SSs is their placement within
475 an ICE (Coyne et al. 2016). Previous studies show these can be exchanged between species
476 within the gut of an individual human or mouse, suggesting selection for compatibility among
477 the effector repertoires they encode (Coyne et al. 2014, Garcia-Bayona et al. 2021, Sheahan et al.
478 2024). However, the factors governing the extent to which the ICE-encoded T6SSs spread
479 among co-resident *Bacteroides* species are not well understood. We show using ICE-seq that an
480 ICE-encoded GA1 T6SS is present in a minority of *Bacteroides* species within the gut of a
481 natural mouse community. The ICE present in two species, *B. acidifaciens* and *B. caecimuris,*
482 shares >99% sequence identity across the element, indicated it was recently exchanged between
483 them. Interestingly, we find that T6SS activity contributes to *B. acidifaciens* competitiveness

484 towards *B. caecimuris* during co-colonization of gnotobiotic mice, suggesting these species may
485 occupy a similar niche, and thus be in direct competition in their native habitat. Accordingly,
486 ICE acquisition by one of these species could be expected to exert strong selective pressure for
487 acquisition and retention of the element in the second species, allowing it to resist intoxication by
488 its competitor.

489 In contrast, we find that *P. vulgatus* has not acquired the T6SS-encoding ICE in the
490 WildR gut community. We show that the T6SS is active in this species, and it can promote initial
491 gut colonization by *P. vulgatus*. However, during stable gut colonization, the fitness cost of
492 harboring the element appears to outweigh its benefit. One potential explanation for these results
493 is that *P. vulgatus* relies on mechanisms other than T6SS-mediated antagonism to maintain its
494 niche in the gut. An alternative possibility is that the fitness cost incurred by T6SS expression in
495 *P. vulgatus* is higher than in species that maintain the element, such as *B. caecimuris* and *B.*
496 *acidifaciens*. In support of this, we observed that T6SS activity provided up to a 100-fold
497 competitive advantage over two days to *P. vulgatus* during growth in competition with WildR
498 Bacteroidales isolates, whereas in *B. acidifaciens,* the degree of T6SS-dependent
499 competitiveness was considerably more modest (up to five-fold). This difference suggests that *P.*
500 *vulgatus* may lack a regulator that modulates the activity of the T6SS in *B. acidifaciens,* thus
501 increasing the cost of producing the system in this species. This observation is in-line with a
502 proposal by Comstock and colleagues that dysregulation is a factor limiting GA1 and GA2
503 mobility within communities (Garcia-Bayona et al. 2021). Whether other factors contribute to
504 the differences in the fitness costs and benefits conferred by ICE acquisition across species
505 remains to be determined.

506 Our finding that the T6SS of a gut *Bacteroides* species is important for stable
507 colonization of its native habitat expands the diversity of demonstrated benefits to T6SSs in
508 natural environments. In both the midgut of honeybees and the light organ of bobtail squid, the
509 T6SS appears to be primarily important for intraspecies competition (Speare et al. 2018, Motta et
510 al. 2024). Strains of the squid symbiont *Vibrio fischeri* encoding a T6SS exclude T6SS-deficient
511 competitors from the light organ crypts they colonize (Speare et al. 2018). Similarly, T6SS-
512 encoding honeybee gut resident *Snodgrassella alvi* excludes T6SS-deficient strains from bee gut
513 colonization (Motta et al. 2024). In contrast, the T6SS of *Pseudomonas* species appears to be
514 important for colonization of soil and the plant roots, and one study found that T6SS activity of
515 *P. protegens* affected overall community composition in the tomato rhizosphere (Duran et al.
516 2021, Vazquez-Arias et al. 2025). Additional studies across more habitats and species will serve
517 to build a complete picture of the ecological and evolutionary factors that have led to the
518 dissemination of the T6SS across such a wide diversity of species.
519 A key challenge facing the field of microbiome research is how to investigate gut
520 microbe functions of interest in a physiologically relevant context that recapitulates the
521 complexity of native gut communities. In this study, we have developed a number of resources
522 and methods to facilitate the use of WildR-colonized mice as a model microbiome composed of
523 co-evolved species native to the murine gut environment. We have isolated 16 species from the
524 community, and obtained genomes representing 55% of the phylogenetic diversity of the
525 community. Our finding that the carrying capacity of the WildR community can be exploited to
526 facilitate functional replacement of endogenous strains with modified derivatives is a
527 generalizable method that can be used to answer questions unrelated to T6S or interbacterial

528 antagonism. These resources and methods should further encourage adoption of the WildR

529 community as a valuable tool for advancing mechanistic gut microbiome research.

530

Acknowledgements

We thank Ben Ross and members of the Mougous lab for helpful discussions, Stephan Rosshart for providing access to individual wild mouse microbiome data, Natasha Bencivenga-Barry for assistance with preparation of WildR cryopreserved stocks, the Microbial Interactions & Microbiome Center for providing laboratory space and equipment to support animal studies, and the UW Gnotobiotic Animal Core for assistance with gnotobiotic animal work including experimental design, breeding, and technical expertise. This work was supported by NIH grant R35GM118159 (to A.L.G) and NIH grant R01 DE027850 (to C.D.J). B.A.S. was supported by a Ruth R. Kirschstein National Research Service Award (F32 AI164853). J.D.M is a Howard Hughes Medical Institute Investigator and held the Lynn and Michael Garvey Chair in Gastroenterology at the University of Washington. J.D.M. currently holds the John F. Enders Professorship at Yale University.

544 **Figure Legends**

545 **Figure 1. The WildR murine gut microbiome is stable over multiple generations and**

546 **harbors an ICE-encoded T6SS**

547 (A) Phylum-level taxonomic composition of the WildR or lab-derived murine gut microbiome at

548 different generations. Data from the initial wild-caught donor mice (Wild), the WildR F2

549 generation and the lab mice-derived community derive from new analysis of previously

550 published sequencing data (Rosshart et al. 2017). WildR F7 data derives from two cryopreserved

551 samples of pooled ilocecal contents (A, B) and fecal pellets from two mice (1, 2) used to

552 propagate the community. *indicates technical duplicate samples. Source data is presented in

553 Supplemental Table 1. (B-E) Comparison of the abundance of the 100 genera most prevalent in

554 wild donor mice between the indicated communities. Points are shaded to show overlapping

555 datapoints (darker shades), and Spearman's correlation for each comparison is indicated (ρ). ND,

556 not detected. (F) To-scale schematic depicting the *Bacteroides acidifaciens* T6SS gene cluster.

557 (G) Bioinformatic domain predictions for T6SS effector and immunity proteins of *B.*

558 *acidifaciens*. Conserved amino acids are indicated in bold.

559

560 **Figure 2. The *B. acidifaciens* T6SS intoxicates other WildR Bacteroidales species.**

561 (A) Normalized growth yield (final/initial CFU, mean ± SD) of the indicated strains of *B.*

562 *acidifaciens* (recipients) after *in vitro* growth in competition with *B. acidifaciens* wild-type or

563 Δ*tssC* (donors). Data are representative of at least three biological replicates. *$p \leq 0.05$ (two-

564 tailed t-test). CFU, colony forming units; *bae, e; bai, i*. (B) Mean (± SD) relative fitness of wild-

565 type *B. acidifaciens* relative to a Δ*tssC* derivative during *in vitro* growth competition assays with

566 the indicated species isolated from the WildR community. Data represent 3 biological replicates.

567 *indicates the T6SS is significantly important for competitiveness (unpaired two-tailed t-test. $p <$
568 0.05). (C) Abundance (% reads per kilobase per million) of WildR species in two initial wild-
569 caught donor mice used to establish the WildR (Rosshart et al. 2017). (D) Abundance of *B.*
570 *acidifaciens* Δ*bae1* Δ*bai1* Δ*bae2* Δ*bai2* in mouse fecal samples collected following co-gavage of
571 germ-free mice with this strain and wild-type or T6SS-inactivated (Δ*tssC*) *B. acidifaciens.* ND,
572 not detected. *$p < 0.05$ (mixed-model ANOVA with repeated measures and Šidák's multiple
573 comparisons tests) (E) Relative abundance (compared to total *Bacteroides*) of *B. caecimuris* F5
574 following co-gavage of germ-free mice with *B. acidifaciens* wild-type or Δ*tssC*. *$p < 0.05$ (two-
575 way ANOVA with repeated measures and Šidák's multiple comparisons tests). For D and E, n=6
576 mice from two independent replicates. Boxplots represent the interquartile range and mean for
577 each condition; whiskers represent minimum and maximum detectable values; points represent
578 individual values.
579
580 **Figure 3. Maintenance of *B. acidifaciens* in the WildR community is mediated by the T6SS**
581 (A) Schematic of approach to exploit the carrying capacity of the mouse gut to promote modified
582 strain engraftment during WildR microbiome establishment without affecting community
583 structure. Left, design of proof-of-concept experiment to evaluate the effect of increasing the
584 amount of *B. acidifaciens* relative to the amount of the WildR microbiome during oral gavage.
585 Right, design of experiment to evaluate the importance of the T6SS for *B. acidifaciens* fitness in
586 the WildR microbiome-colonized mouse gut. (B-D) Analysis of total (B), or introduced (C,D) *B.*
587 *acidifaciens* populations in gavage (Day 0) or post-gavage fecal samples from germ-free mice
588 colonized with the WildR and variable levels of *B. acid* ^{exo}. B) Total abundance of *B.*
589 *acidifaciens* calculated from sequencing 16S rRNA genes amplified from DNA extracted from

590 fecal samples. Differences in *B. acidifaciens* abundance across mice gavaged with different
591 amounts of *B. acid* ^{exo} was not significant (n=4 mice/sample, mixed-effects analysis). C) Relative
592 abundance of *B. acid* ^{exo} in the indicated fecal samples compared to total *B. acidifaciens* as
593 determined by qPCR. D) Abundance of *B. acid* ^{exo} in the indicated fecal samples as determined
594 by plating for CFU on selective media. (E) Principal coordinate analysis of weighted Unifrac
595 diversity metrics calculated from 16S rRNA gene amplicon sequencing data from feces collected
596 from mice colonized with the WildR and variable amounts of *B. acid* ^{exo}. (F-H) Quantification of
597 *B. acid* ^{exo} (F,G) or total (H) *B. acidifaciens* population in gavage (Day 0) and post-gavage fecal
598 samples from germ-free mice colonized with the WildR community and 10-fold excess wild-type
599 or Δ*tssC B. acid* ^{exo}. n=8 mice per strain, across two biological replicates. (F) CFU quantification
600 of *B. acid* ^{exo} and *B. acid* ^{exo} Δ*tssC* . *$p \leq 0.05$ (two-way ANOVA with repeated measures and
601 Šidák's multiple comparisons test). (G) Abundance of *B. acid* ^{exo} or *B. acid* ^{exo} Δ*tssC* relative to
602 the total *B. acidifaciens* population, as determined by qPCR. *$p \leq 0.05$ (two-way ANOVA with
603 repeated measures and Šidák's multiple comparisons test). (H) Total abundance of *B.*
604 *acidifaciens,* calculated from 16S rRNA gene amplicon sequencing. Samples from mice
605 colonized by the WildR community alone (no *B. acid* ^{exo}, white bars) are included for
606 comparison. Differences in *B. acidifaciens* abundance based on *B. acid* ^{exo} genotype were not
607 significant (mixed-model ANOVA test). For panels B-D and F-H, boxplots represent the
608 interquartile range with indicated mean for each condition, whiskers represent maximum and
609 minimum detectable values, and points show values from individual mice.
610
611 **Figure 4. *P. vulgatus* gains a limited fitness benefit from the T6SS-encoding ICE in WildR-**
612 **colonized mice.**

613 (A) Frequency of mapped ICE junctions deriving from the indicated species as determined by 5′
614 or 3′ ICE-Seq analysis of DNA extracted from fecal samples collected either 7 or 14 days post-
615 gavage of the WildR into germ-free mice (n=4). Mice housed in separate or shared cages are
616 indicated. (B) Relative competitive index from *in vitro* growth competitions between *P. vulgatus*
617 ICE or ICE Δ*tssC* and recipient strains isolated from the WildR microbiome (Pseudomonadata,
618 grey; Bacteroidota, green). The mean ± SD from three biological replicates is shown. Asterisks
619 indicate recipient species for which the difference in competitive index was statistically
620 significant between donor strains ($p<0.05$, unpaired two-tailed t-test). (C) Recovery of *P.*
621 *vulgatus* strains containing the indicated versions of the ICE after *in vitro* growth with *B.*
622 *acidifaciens*. The mean ± SD from one biological replicate and its associated technical replicates
623 are shown, which represent results from at least three biological replicates. *$p \leq 0.05$ (two-tailed
624 t-test). *bae, e; bai, i*. (D) Abundance of wild-type *P. vulgatus* in feces collected from mice (n=4)
625 co-colonized with *P. vulgatus* ICE or *P. vulgatus* ICE Δ*tssC*. Boxplots represent the interquartile
626 range with indicated mean for each condition, whiskers represent minimum and maximum
627 values, points show values from individual mice. *$p \leq 0.05$ (two-way ANOVA with repeated
628 measures test and Šidák's multiple comparisons test). (E) Schematic of experimental design to
629 test the fitness of *P. vu*l ^{exo} + T6SS-ICE in the WildR community. (F) Recovery of *P. vul* ^{exo} +
630 ICE (dark blue) or *P. vul* ^{exo} + ICE Δ*tssC* (light blue) from post-gavage fecal samples of mice co-
631 colonized with the WildR community as depicted in (E). Boxplots represent the interquartile
632 range with indicated mean for each condition, whiskers represent minimum and maximum
633 values, points show values from individual mice. Data in panel F is from two biological
634 replicates with 4 mice per group per replicate (n=8). *$p < 0.05$ (two-way ANOVA with repeated

635 measures and Šidák's multiple comparisons test to compare *P.vulgatus* ICE and ICE Δ*tssC*

636 populations), † $p < 0.05$ (unpaired t-test to compare day 7 and day 56 samples).

637

638 **Supplemental Figure 1. Evidence supporting stability of the WildR microbiome over**

639 **multiple generations and identification of an ICE-encoded T6SS**

640 (A) Schematic depicting the generation of the WildR F7 cryoprserved stocks from the combined

641 cecal contents of six mice used to propagate the community, and subsequent community

642 characterization steps. (B-C) Comparison of the abundance of the 100 genera most prevalent in

643 wild donor mice between the indicated communities. Points are shaded to show overlapping

644 datapoints (darker shades), and Spearman's correlation for each comparison is indicated (ρ). ND,

645 not detected. (D) Mapping efficiency of metagenomic reads from different WildR community

646 generations to selected murine-derived genome databases: the WildR catalog (86 MAGs and

647 genomes from the WildR, generated in this study) or the comprehensive mouse microbiota

648 genome catalog (CMMG; 1573 species across mouse microbiomes (Kieser et al. 2022)). (E) To-

649 scale schematic of the ICE containing the GA1 T6SS encoded in *B. acidifaciens* and *B.*

650 *caecimuris* F12. Location of single base deletion in *B. caecimuris* F12 highlighted in the orange

651 box.

652

653 **Supplemental Figure 2. Activity of the *B. acidifaciens* T6SS against species co-resident in**

654 **the WildR community.**

655 (A) *In vitro* mating efficiency of the integrative plasmid pNBU2-*ermG:: tssC* into *B.*

656 *acidifaciens*. "RM silent" indicates plasmid was mutated to remove a *B. acidifaciens* methylated

657 motif. Data shown are mean ± SD from 3 independent matings. N.D., not detected; D.L.,

658 detection limit. (B) Recipient abundance after *in vitro* growth competitions between *B.*
659 *acidifaciens* donors lacking various structural components of the T6SS and the indicated
660 recipient species. (C) Competitive index from *in vitro* growth competition between indicated
661 WildR isolates (recipient) and *B. acidifaciens* donors. For B & C, data show the mean ± SD of
662 technical replicates from one biological replicate and represent results from at least three
663 biological replicates. *$p \leq 0.05$ by two-tailed t-test; all other comparisons were not significant.
664 (D) *B. caecimuris* F5 abundance in cecal contents from germ-free mice co-colonized with *B.*
665 *acidifaciens* wild-type or Δ*tssC*. Data show the mean ± SD and points indicate values from
666 individual mice (n=6) across two biological replicates. *$p \leq 0.05$ (two-tailed t-test). (E) *P.*
667 *vulguatus* abundance in feces from germ-free mice (n=6, two biological replicates) co-colonized
668 with *B. acidifaciens* wild-type or Δ*tssC* and *P. vulguatus*. Boxplots represent the interquartile
669 range with indicated mean for each condition, whiskers represent minimum and maximum
670 values, points represent individual values. *$p \leq 0.05$ (two-way ANOVA with repeated measures
671 test and Šidák's multiple comparisons test). (F) *P. vulguatus* abundance in cecal contents from
672 mice described in panel E. Data show the mean ± SD and points show values from individual
673 mice (n=6). No statistical difference was found based on *B. acidifaciens* genotype by two-tailed
674 t-test. (G) Relative abundance (% reads per kb per million) of selected WildR Bacteroidales
675 species in the WildR F7 generation. Data are mean + SD from cryopreserved WildR stocks and 2
676 fecal samples from mice used to propagate the WildR F7 community.
677
678 **Supplemental Figure 3. Addition of *B. acid* ^{exo} to the WildR does not alter community**
679 **composition and enables *in situ* measurement of T6SS-mediated fitness.**

680 (A,B) Recovery of *B. acid* ^{exo} from feces (A) and cecal contents (B) following gavage of germ-
681 free mice with the WildR community and the indicated amount of *B. acid* ^{exo} relative to the
682 endogenous population. (C,D) Recovery of *B. acid* ^{exo} or *B. acid* ^{exo} Δ*tssC* from feces (D) or
683 cecal contents (E) from mice colonized with the WildR and *B. acid* ^{exo} strains. *$p \leq 0.05$ (two-
684 way ANOVA with repeated measures test and Šidák's multiple comparisons test in C, unpaired
685 t-test in D). For data in panels A-D, boxplots represent the interquartile range with indicated
686 mean for each condition, whiskers represent minimum and maximum values, and points show
687 values from individual mice. (E) Principal coordinate analysis of weighted Unifrac diversity
688 metrics calculated from 16S rRNA amplicon sequencing data from feces collected from mice
689 colonized with the WildR alone or in combination with the indicated strain of *B. acid* ^{exo}. Gavage
690 samples highlighted in pink and remaining timed fecal and cecal (collected at 56 days post
691 gavage) samples are colored as indicated. Data shown are from one biological replicate,
692 representative two experiments conducted.
693
694 **Supplemental Figure 4. Distribution of the T6SS-ICE in the WildR suggests limited fitness**
695 **benefit to some *Bacteroides* sp.**
696 **(**A) Schematic of ICE-seq approach to identify WildR species encoding the ICE. The junction
697 amplification and sequencing strategy applied to both ends of the ICE is depicted only for the 3′
698 end for simplicity. (B) Schematic depicting ICE transfer from *B. acidifaciens* (marked with Cm^R)
699 to *P. vulgatus* (marked with Erm^R) via *in vitro* conjugation and selective plating. (C) To-scale
700 schematic of ICE insertion sites in *P. vulgatus* ^{exo} + ICE transconjugants that acquired the
701 indicated versions of the ICE. (D) Abundance (relative to total *P. vulgatus*) of the indicated *P.*
702 *vulgatus* ^{exo} in fecal samples from mice co-colonized with the WildR community, as determined

703 by qPCR. Boxplots represent the interquartile range with indicated mean for each condition,
704 whiskers represent minimum and maximum values, and points show values from individual mice
705 (n=8) from two biological replicates. Asterisks indicate significant differences between *P. vul* ^{exo}
706 + ICE and *P. vul* ^{exo} + ICE Δ*tssC* frequency at the indicated time points ($p<0.05$, Šídák's multiple
707 comparisons test, mixed model ANOVA with multiple comparisons). N.D., not detected. (E)
708 Principal coordinate analysis of weighted Unifrac diversity metrics calculated from 16S rRNA
709 gene amplicon sequencing data from feces collected from mice (n=8/group across 2 biological
710 replicates) colonized with the WildR and either *P. vul* ^{exo} + ICE (closed circles) or *P. vul* ^{exo} +
711 ICE Δ*tssC* (open circles). The community composition varied between groups at early time
712 points (purple; Rep 1, $p=0.021$, pseudo-F=2.7; Rep 2, $p=0.011$, pseudo-F=12, PERMANOVA
713 test), but varied less or not signifcantly at late time points (orange; Rep 1, $p=0.25$, pseudo-F=1.3;
714 Rep 2, $p=0.003$, pseudo-F=5).
715
716

717 **Methods**

718 **Strains and culture conditions**

719 Strains employed in this study are listed in Supplemental Table 5. *E. coli* strains employed
720 include *E. coli* EC100D pir+ (for cloning), and *E. coli* S17-1 λpir and *E. coli* S17-1 λpir +
721 RK231 (for conjugation into Bacteroidales sp.). *E. coli* was grown aerobically at 37 ˚C in LB.
722 Other bacterial strains employed in this study were isolated from the WildR community as
723 described below. Isolates and their culture conditions are listed in Supplemental Tables 5 and 6.
724 A hard-sided anaerobic workstation (Don Whitley Scientific) containing 10% CO_2, 10% H_2, and
725 80% N_2 was used for all anaerobic microbiology procedures. If required, antibiotics were
726 supplemented at the following concentrations: 25 µg erythromycin (erm)/mL, 200 µg gentamicin
727 (gent)/mL, 25 µg chloramphenicol (cm)/mL, and 100 ng anhydrotetracycline (aTc)/mL.

728

729 **Generation of WildR reference stocks**

730 Cryoperserved stocks of the WildR microbiome were prepared as previously described
731 with modifications as described below (Rosshart et al. 2017). All procedures were approved by
732 the Yale University Institutional Animal Care and Use Committee (IACUC). Male and female 6-
733 8 week old mice were housed in as singles or pairs in flexible plastic gnotobiotic isolators with at
734 12-hr light/dark cycle. Mice were a provided standard chow (5K67 LabDiet; Purina) and water
735 ad libitum. Frozen ileo-cecal contents from mice colonized with the F6 generation of the WildR
736 microbiome were obtained from Taconic Biosciences
737 (https://www.taconic.com/services/microbiome/wild-mouse-microbiome). To propagate this
738 community, six germ-free C57BL6 mice were inoculated with the WildR microbiome by oral
739 gavage (100 µL/mouse) on two consecutive days. Fecal samples were collected 14 days after

740 gavage. After 14 days post gavage, fecal samples were collected for downstream
741 characterization, mice were euthanized and transferred to an anaerobic chamber. The contents of
742 the ileum, cecum, and colon ("gut") were collected and pooled from each mouse. Pooled gut
743 contents were diluted in pre-reduced, sterile PBS-C (PBS pH 7.4 with 1% cysteine) at 15 mL/g
744 gut contents before passing through a 70 µm cell strainer. Material was then diluted in an equal
745 volume of storage buffer (PBS-C with 40% glycerol final concentration), aliquoted into Wheaton
746 vials to maintain an anerobic environment, and stored at -80 ˚C.
747
748 **Metagenomic sequencing of the WildR community**
749 For shotgun sequencing on the Illumina platform, genomic DNA was extracted from two
750 aliquots of the propagated, cryopreserved WildR stock (~250 mg of pelleted cells) and fecal
751 pellets (~50 mg) from two of the six mice inoculated with the Taconic WildR material using the
752 MoBio PowerFecal DNA Isolation kit (Catalog #12830-50, MoBio Laboratories, California,
753 USA). Sequencing libraries were prepared using an in-house protocol (Salipante et al. 2014) and
754 sequenced on the Illumina NextSeq using the NextSeq 500/550 Highoutput kit v2.5 300 cycles
755 (Cat # 20024908). Samples were processed in technical duplicates to correct for PCR errors.
756 Raw reads have been deposited with links to BioProject PRJNA1367654 in the NCBI database.
757 For long-read sequencing (Oxford Nanopore MinION), high-molecular weight (HMW)
758 gDNA was extracted from ~500 µL of the WildR cryopreserved stock using the Qiagen
759 Genomic-tip 20/G (Cat#13323) following the protocol for bacterial DNA extraction, except 5 µL
760 of Qiagen lytic enzyme (catalog #158928) and 10 µL of MetaPolyzme (Millipore Sigma
761 MAC4L-5MG resuspended in 750 µL of water) were added instead of lysosome for more
762 efficient enzymatic lysis of diverse bacteria in the community (Maghini et al. 2021). HMW DNA

763 was then cleaned and concentrated with an isopropanol precipitation as described and eluted in
764 100 µL of water as previously described (Maghini et al. 2021). DNA was incubated at 55 ˚C for
765 1 hr before placing at 4 ˚C for 3 days to increase resuspension of HMW gDNA fragments.
766 Quality and quantity of HMW gDNA were assessed by NanoDrop UV-Vis spectroscopy and
767 Qubit dsDNA HS fluorimetry assay (Cat# Q33231), respectively, and the presence of fragments
768 >10 kb was confirmed by agarose gel electrophoresis. Libraries for sequencing using the Oxford
769 Nanopore MinION were prepared using the Oxford Nanopore SQK-LSK110 kit and 902 ng of
770 WildR HMW gDNA as the starting material. The sequencing library was loaded onto a R9.4.1
771 SpotON flow cell and run for 74 hrs on the Mk1C until ~50 pores remained. The run resulted in
772 22 Gb of sequencing data from 8.6 million reads with an N50 of 5.3 kb. Raw reads have been
773 deposited with links to BioProject PRJNA1367654 in the NCBI database.
774
775 **Taxonomic classification of WildR-derived metagenomic sequences**
776 Metagenomic reads, generated from Illumina sequencing of either WildR reference
777 stocks or fecal samples from mice 14 days post gavage with cecal contents from Taconic, were
778 cleaned to remove adapter sequences using Trimmomatic (v0.39) (Bolger et al. 2014) and any
779 reads mapping to the mouse (*Mus musculus*) genome (RefSeq GCF_000001635.27) using
780 bowtie2 (Langmead and Salzberg 2012). Taxonomic classification of each read was performed
781 using a publicly available custom Kraken2-Bracken Snakemake pipeline based on the
782 comprehensive mouse microbiota genome catalog (CMMG; (Lu et al. 2017, Wood et al. 2019,
783 Kieser et al. 2022) https://github.com/SilasK/Krak). To ensure high fidelity alignment, the
784 pipeline was modified to include a confidence of 0.51 in the Kraken2 command, and a threshold
785 of 1000 reads per sample was applied to the Bracken analysis. The same classification pipeline

786 was applied to metagenomic sequencing data from other WildR generations and lab mice
787 previously published by Rosshart and colleagues (Rosshart et al. 2017). Classifications were
788 condensed at the order and genus levels for downstream analyses.
789
790 **Metagenome assembly**
791 WildR metagenome-assembled genomes (MAGs) were generated from Illumina and
792 MinION reads using the MUFFIN 1.0.6 pipeline ((Van Damme et al. 2021);
793 https://github.com/RVanDamme/MUFFIN). Briefly, short and long reads were filtered for high-
794 quality before performing hybrid assembly with MetaFlye (version 2.7;
795 https://github.com/mikolmogorov/Flye). Instead of the default polishing step using Pilon, we
796 modified the MUFFIN pipeline to reduce error by using Polypolish for short read polishing of
797 our assemblies ((Wick and Holt 2022); https://github.com/rrwick/Polypolish). Binning was
798 performed with Concot (version 1.1.0) (Alneberg et al. 2014) , Metabat2 (version 2.13) (Kang et
799 al. 2019), and Maxbin2 (version 2.2.7, https://sourceforge.net/projects/maxbin2/), and refined by
800 metawrap (version 1.2.2) (Uritskiy et al. 2018). Hybrid reassembly was then performed with
801 Unicycler (version 0.4.7) (Wick et al. 2017). Bin quality was determined using CheckM (version
802 1.0.13) (Parks et al. 2015) and taxonomic classification was performed with GTDB-tk (version
803 2.1.0) (Chaumeil et al. 2019) . Finally, all genomes were annotated with Prokka (version 1.12)
804 (Seemann 2014). The assembly details and quality for each MAG are listed in Supplemental
805 Table 2. MAG sequences are available at https://doi.org/10.5281/zenodo.17716312.
806
807 **WildR isolate collection and identification**

808 Media used for cultivation of isolates from the WildR community include supplemented
809 Brucella-blood agar [BBL ™ Brucella broth (BD Cat#90000-076), 50 mg hemin/L, 0.5 mg
810 menadione/L, and 5% defibrinated horse blood], Tryptone Yeast Extract Glucose (TYG)
811 Medium (20g tryptone/L, 10g yeast extract/L, 5 g glucose/L, 1 g cysteine/L, 71 µM $CaCl_2$, 78
812 µM $MgSO_4$, 0.3 mM KH_2PO_4, 0.3 mM K_2HPO_4, 1.4 mM NaCl, 5 mg hemin/L, and 0.2%
813 $NaHCO_3$) (Bacic and Smith 2008), BHIS-FBS [Brain heart infusion (BHI) powder supplemented
814 with 5 mg hemin/L, 0.2 mg menadione/L, 0.5 g cysteine/L, and 10% fetal bovine serum], BHIS-
815 blood agar (BHI supplemented with 5 mg hemin/L, 1 g cysteine/L, 0.2% $NaHCO_3$, 5%
816 defibrinated horse blood, and 1.5% agar), Columbia-blood agar [Columbia broth powder (BD
817 #294420) supplemented with 0.5 mg menadione/L and 5% defibrinated horse blood], MRS
818 [MRS broth (BD #288130), supplemented with 1.5% agar if required], YCFAC [Yeast casitone
819 fatty acids with carbohydrates broth (#AS-680) or agar (#AS-675) purchased from Anaerobe
820 Systems], and BG [23.1 g Bryant and Burkey Medium (BB)/L (Sigma Aldrich #91903) and 12.5
821 g modified Gifu Anaerobic Medium (mGAM)/L (Himedia Laboratorires #M2079), which is a
822 70:30 ratio of BB:mGAM] (Javdan et al. 2020). All media was degassed for at least 24 hours
823 before culturing.
824 Dilutions of the WildR reference stock or fresh fecal pellets collected from WildR-
825 colonized mice resuspended in PBS were plated on anaerobic media and incubated anaerobically
826 at 37 ˚C for 2-4 days. Single colonies were picked and used to inoculate broth cultures or were
827 restruck on fresh plates and incubated at 37 ˚C anaerobically for 2 days. For storage, sterile, pre-
828 reduced 50% glycerol was added to cultures, and the mixture was stored at -80 ˚C. Cultures were
829 then screened for taxonomic identity by full-length 16S rRNA gene or *gyrB* gene sequencing
830 (primer sequences provided in Supplemental Table 5. Target genes were amplified from ~2 µL

831 of cultured cells resuspended in 20 µL TE (10 mM Tris, pH 8; 1 mM EDTA). PCR products
832 were cleaned up with Exo-SAP-IT (ThermoFisher, Catalog # 78201.1.ML) and then sequenced
833 by Sanger sequencing. Resulting reads were trimmed and assigned putative taxonomy using
834 blastn against the 16S ribosomal RNA sequences (Bacteria and Archea) database (Altschul et al.
835 1990). After initial screening, representative cultures from each species identified were subjected
836 to an additional round of strain purification by streaking for single colonies, and species identity
837 was reconfirmed by Sanger sequencing of the full-length 16S rRNA gene amplicons. Strains
838 isolated and their growth conditions are listed in Supplemental Table 6.
839

840 **Whole genome sequencing of WildR isolates**

841 De novo genome sequencing of WildR isolates was performed using a combination of
842 short (Illumina) and long-read sequencing. High molecular weight gDNA was extracted from
843 *Bacteroidales* sp. using the Qiagen genomic tip (20/G) kit following the standard protocol for
844 Gram-negative extraction. The HMW DNA extraction kit from NEB (#T3060) was used for
845 extracting HMW gDNA from *L. murinus* following the standard input protocol except the lysis
846 buffer contained 5 µL of Qiagen lytic enzyme (catalog #158928) and 10 µL of metapolyzme
847 (Millipore Sigma MAC4L-5MG resuspended in 750 µL of water). HMW gDNA was extracted
848 from *L. reuteri* and *L. johnsonii* using the Promega Wizard HMW DNA Extraction kit (#A2920).
849 For *M. intestinale*, *M. gordoncarteri*, *S. musculi*, and *D. freteri*, gDNA was extracted with
850 mechanical lysis and column clean up. To lyse cells, 500 µL of PB (Qiagen), 250 µL 20% SDS,
851 550 µL of phenol:chloroform:isoamyl alcohol (24:24:1), and ~250 µL of 0.1-mm-zirconia-silica
852 beads were added to ~$2x10^9$ cells. Cells were then mechanically lysed with bead beating (RT, 1
853 min at high speed, 2 cycles) (BioSpec). Genomic DNA was further purified using columns from

854 the Qiagen Blood and Tissue kit (#69504) and washed following the standard protocol.
855 Extraction of genomic DNA from modified *B. acidifaciens* and *P. vulgatus* clones for
856 resequencing was performed using the Qiagen Blood & Tissue kit (#69504) following the
857 protocol for Gram-negative bacteria. For all gDNA extractions, the quality and size of gDNA
858 was assessed by Qubit, nanodrop, and agarose gel electrophoresis before library prep.
859 Libraries for short-read whole genome sequencing were prepared with the Illumina DNA
860 prep kit (catalog #20018704), multiplexed using barcoded adapters purchased from IDT (IDT for
861 Illumina DN/RNA UD Indexes SetA, Catalog #20027213), and sequenced on either the Illumina
862 iSeq or the MiniSeq, which included a 5% PhiX spike-in, to obtain paired-end reads (2x150 bp).
863 To facilitate generation of closed genomes, *Bacteroidales* and *Lactobacillales* spp. were also
864 sequenced on the Oxford Nanopore MinION. Libraries for long-read sequencing were prepared
865 using LSK-110 with modifications to include ligation of barcodes (EXP-NBD104) following the
866 protocol described for the LSK-109 kit. Briefly, DNA was repaired following the LSK-110
867 protocol using NEB buffers. Then, barcodes were ligated using Blunt/TA ligase following steps
868 described for the LSK-109 kit. Finally, after barcode ligation, adapter sequences were ligated as
869 described for LSK-110. The sequencing library was loaded onto a R.9.4.1 SpotON flow cell and
870 run on the Mk1C until ≥ 200,000 reads were collected for each sample. If more reads were
871 required, the flow cell was washed, and more libraries were loaded.
872 For *Bacteroidales* and *Lactobacillales* spp., genomes were assembled from long reads
873 using Trycycler (v0.5.3, (Wick et al. 2021)). Briefly, reads were subsampled and assembled with
874 either Flye (v2.9-b1768; (Kolmogorov et al. 2019)), Miniasm (v0.3-r179)+Minipolish (v0.1.2)
875 (Wick and Holt 2019), or Raven (v1.8.1; https://github.com/lbcb-sci/raven) before combining
876 similar assemblies to generate a single consensus sequence as described in the Trycycler wiki

877 (https://github.com/rrwick/Trycycler/wiki). Assemblies were polished with Illumina reads using
878 Polypolish (version 0.5.0; (Wick and Holt 2022)) and Pilon (version 1.24; (Walker et al. 2014)).
879 For *Phocaeicola vulgatus*, genomes were assembled using the hybrid assembly feature in
880 Unicycler (version 0.4.8; (Wick et al. 2017)). Finally, genomes were annotated with Prokka
881 (version 1.14.6; (Seemann 2014)). For other species, adapters were removed from reads using
882 BBDuk (version 38.84) in Geneious Prime (2024.0.5) (https://www.geneious.com), and then
883 genomes were assembled with the Geneious assembler. For genomes deriving from modified
884 clones of *B. acidifaciens* and *P. vulgatus,* spontaneous mutations were determined by aligning
885 short reads to assembled genomes from the parental strains using BreSeq (Deatherage and
886 Barrick 2014). Genome and assembly metrics for each isolate genome are listed in
887 Supplemental Table 2, and all genomes have been deposited with links to BioProject
888 PRJNA1367654 in the NCBI database.
889
890 **Determining the abundance of species in the WildR community**
891 Abundance of species for which we had obtained a genome sequence (MAG or isolated-
892 derived) was assessed by quantifying the frequency of metagenomic sequencing reads mapping
893 to the genome of interest. Cleaned short, metagenomic reads from either wild donor, F2 WildR
894 mice (Rosshart et al. 2017) or F7 WildR cryopreserved stocks were mapped to a catalog
895 containing WildR F7 MAGs and isolate genomes using BWA-MEM
896 (https://arxiv.org/abs/1303.3997), retaining only correctly paired read alignments using samtools
897 (Li et al. 2009). Reads for all contigs in a MAG or isolate genome were summed and the
898 percentage of reads per kilobase per million reads was calculated. For each sample, the total
899 reads mapping to this catalog was retrieved using samtools flagstat. The same metagenomic

900 reads were also mapped to all genomes in the CMMG catalog (https://ezmeta.unige.ch/CMMG/)
901 using the same BWA-MEM command.
902
903 **Identification and bioinformatic characterization of an ICE-encoded T6SS in WildR**
904 **genomes**
905 To identify T6SS gene clusters present in WildR strains, we first searched for genes
906 annotated to encode T6SS-related functions in the genomes of Bacteroidales isolates from the
907 community. This led to the identification of candidate T6SS gene clusters in strains of *B.*
908 *acidifaciens* and *B. caecimuris.* Blastp searches against the NCBI non-redundant protein
909 sequence database with each of the candidate T6SS genes in the clusters found that each
910 predicted T6SS component shares ≥80% identity with previously characterized T6SS proteins in
911 other Bacteroidales species, and confirmed that the gene clusters contain the complete
912 compliment of genes required to constitute a functional T6SS[iii] (Altschul et al. 1990, Russell et
913 al. 2014, Coyne et al. 2016). Putative effector genes were identified based on proximity of genes
914 to the T6SS structural genes (e.g., VgrG) and the presence of N-terminal domains associated
915 with T6SS effectors (e.g., PAAR). Effector activity of the C-terminal region of candidate
916 effectors (~100 aa) was predicted using CD-Search and Foldseek (Marchler-Bauer et al. 2009,
917 van Kempen et al. 2023). For the later, positive hits from the AFDB50 database were defined by
918 a probability score of 1. Immunity genes were assigned based on proximity to a putative effector,
919 length (<200 a.a.), and presence of immunity domains identified by CD-Search.
920 The boundaries of the 115 kb T6SS-ICE were determined based on loss of 100% identity
921 in a pairwise alignment between the *B. acidifaciens* and *B. caecimuris* F12 T6SS neighboring
922 sequences (Geneious). Putative functions were assigned to each gene based on similar blastp hits

923 (>30% identity) and classified according to functions typically encoded in ICEs (Coyne et al.
924 2014).
925
926 ***B. acidifaciens* methylome identification**
927 For long-read sequencing using Pacific Biosciences (HiFi/SMRT sequencing), high-
928 molecular-weight (HMW) genomic DNA from each isolate was extracted as described above for
929 the Oxford Nanopore workflow. PacBio HiFi libraries were prepared using the SMRTbell
930 Express Template Prep Kit v2.0 (Pacific Biosciences) according to the manufacturer's
931 recommendations for microbial HiFi genome sequencing, starting with 5–10 µg of HMW DNA
932 per sample. Sequencing was performed on a PacBio Sequel II instrument at the Fred Hutchinson
933 Cancer Center, generating circular consensus sequence (CCS) reads. Raw subreads were
934 processed in SMRT Link (v11.0.0.146107), and CCS reads were used as input for the Microbial
935 Assembly workflow, which performs long-read assembly, polishing, and contig finishing. For
936 each genome, assembly statistics, CCS concordance, contiguity, depth of coverage, and base
937 modification metrics were obtained directly from the SMRT Link analysis reports. Methylation
938 analysis was carried out using the Base Modification and Motif Analysis module with default
939 m6A/m4C detection models. Final polished assemblies and methylome calls for all strains (*B.*
940 *acidifaciens*, *B. caecimuris* F12, *B. thetaiotaomicron*, *B. uniformis*, *P. vulgatus*, and *P.*
941 *distasonis*) were exported from SMRT Link and used for downstream comparative analysis.
942 Raw sequences have been deposited with links to BioProject PRJNA1367654 in the NCBI
943 database.
944
945 **Genetic manipulation of *Bacteroides* strains**

946 Standard molecular procedures were employed for creation, maintenance and
947 transformation of plasmids in *E. coli.* The primers, plasmids, and strains designed for this study
948 are listed in Supplemental Table 5. All primers were purchased from Integrated DNA
949 Technologies (IDT) and geneblocks were synthesized by Twist Biosciences. Enzymes such as
950 OneTaq polymerase, restriction enzymes, and Gibson Assembly reagents were purchased from
951 New England Biolabs (NEB). To generate pNBU2-erm-us1311::*tssC*-singleRMsilent, a two bp
952 change was introduced in the GATATC motif found in the plasmid using quickchange. To
953 generate pLGB13-RMsilent and pNBU2-erm-RMsilent::P5E4, all *B. acidifaciens* methylation
954 sites were identified in the parent plasmid by sequence homology (eight and four, respectively)
955 and then single base pair mutations were designed to remove specific motifs. Plasmids were
956 assembled from synthesized geneblocks containing mutations and amplified fragments of
957 unmodified regions using Gibson assembly and validated by whole plasmid sequencing
958 (Plasmidsauraus).
959 Gene knockouts in *B. acidifaciens* using either pSIE1 or pLGB13 derivatives were
960 generated following previously published protocols with the following modifications (Garcia-
961 Bayona and Comstock 2019, Bencivenga-Barry et al. 2020). Briefly, plasmids were mobilized
962 from *E. coli* S17 into *B. acidifaciens* via overnight anaerobic mating at 37 ˚C where *E. coli* was
963 mixed with a 10-fold excess of *B. acidifaciens*. To further improve mating efficiency, *E. coli* S17
964 harboring the RK231 helper plasmid was also included in the mating mixture at equal CFU to *E.*
965 *coli* S17 harboring the plasmid for allelic exchange (Smith et al. 1992). Merodiploids were
966 isolated by plating on selective media, passaged once in BHIS-FBS without antibiotics to allow
967 for plasmid excision, and plated on Brucella-blood supplemented with aTc for counter selection
968 of the plasmid. Resulting colonies were patched onto selective Brucella-blood plates to confirm

969 loss of the plasmid, and the gene disruption of interest was confirmed by colony PCR. For select
970 mutants employed in germ-free mouse colonization experiments, we performed whole-genome
971 sequencing using an Illumina MiniSeq to identify second site mutations, as described above.
972 Strains expressing heterologous copies of *clpV* were generated by cloning *clpV* and an intrinsic
973 terminator from pWW3855 downstream of the P5E4 promoter in pNBU2-ermG-RMsilent::P5E4
974 as previously described (Whitaker et al. 2017).
975 Integration of pNBU2-ermG or derivatives was performed as previously described (Wang
976 et al. 2000, Koropatkin et al. 2008, Whitaker et al. 2017), but with modified mating conditions as
977 indicated above. Resulting transconjugants were selected on Brucella-blood supplemented with
978 gentamycin and erythromycin, colony purified to confirm Erm^R, and stocked.
979
980 **Interbacterial transfer of the GA1 T6SS-encoding ICE**
981 To transfer the T6SS-encoding ICE from *B. acidifaciens* to *P. vulgatus*, we modified
982 previously described methods for spontaneous *in vitro* mobile element transfer (Supplemental
983 Figure 4B; (Ross et al. 2019)). First, we used allelic exchange as described above to insert a
984 chloramphenicol resistance gene under the control of the constitutive P1 promoter in a neutral
985 site in the ICE in *B. acidifaciens*. Then, Cm^R *B. acidifaciens* cells from overnight cultures were
986 mixed with Erm^R *P. vulgatus* cells at a 10:1 ratio (OD_{600} 6) on Brucella-blood plates. Following
987 24-hours of anaerobic co-culture growth, cells were harvested, resuspended in PBS, and plated
988 on Brucella-blood supplemented with chloramphenicol and erythromycin to select
989 transconjugants. Resulting transconjugants were colony purified and whole genome sequencing
990 was performed using the Illumina platform as described above. Resulting reads that aligned to
991 both the ICE and *P. vulgatus* genome, determined using minimap2 were used to identify the ICE

992 insertion sites (Li 2018). Reads generated in this sequencing have been deposited with links to
993 BioProject PRJNA1367654 in the NCBI database.
994
995 ***In vitro* bacterial growth competition assays**
996 For intra- and interspecies growth competition experiments, donor and recipient strains
997 were spread as lawns on plates and incubated anaerobically at 37 ˚C for 24-48 hours. Most
998 *Bacteroides* sp, *Parabacteroides distasonis*, and *Phocaeicola vulgatus* were grown on Brucella-
999 blood plates, except for *B. sp*910578895, which was grown on BHIS-blood. Other media such as
1000 Columbia-agar (*S. musculi*, *M. intestinale*), MRS agar (*L. murinus*), LB agar (*E. fergusonii*), and
1001 YCFAC (*D. freteri*, *M. gordoncarteri*) were used to culture additional recipient species tested
1002 (Supplemental Table 6). Cells were harvested from plates and resuspended in 1 mL PBS, before
1003 measuring the OD_{600} and diluting to OD 20 or OD 0.2 for donor and recipient strains,
1004 respectively. Cell dilutions were combined at a 1:1 ratio (100:1 final donor:recipient ratio), 10
1005 µL of the mixture was spotted onto plates, and mixtures were incubated anaerobically at 37 ˚C
1006 for 16-20 hours. Most assays were performed on Brucella-blood plates supplemented with 3%
1007 agar except for competitions performed on BHIS-blood with 3% agar (*B. sp*910578895 and *E.*
1008 *gallinarum*), Columbia-blood with 3% agar (*S. musculi* and *M. intestinale*), or YCFAC (*M.*
1009 *gordoncarteri*, *D. freteri*). Growth competitions with strict anaerobes (*S. musculi*, *M intestinale*,
1010 *M. gordoncateri*, and *D. freteri*) were performed entirely under anaerobic conditions using pre-
1011 reduced media. After incubation, all cells were harvested and resuspended in 1 mL of PBS.
1012 Quantification of species abundance at the start and end of each assay was performed by
1013 enumerating colony forming units (CFU) or qPCR. CFU enumeration was used to quantify
1014 species abundance for intraspecies (recipients, Em^R) or interspecies (donors, *B. acidifaciens*

1015 Cm^R; recipients *P. vulgatus*, *B. uniformis*, *B. thetaiotaomicron*, *B. caecimuris* F5, *B. caecimuris*
1016 F12, and *P. distasonis*, Em^R or *E. gallinarum* (BHI-blood, aerobic), *L. murinus* (MRS,
1017 anaerobic), or *E. fergusonii* (LB, aerobic)) growth competitions. Interspecies growth
1018 competitions with strict anaerobes, *B. sp*910578895, or *P. vulgatus* donors were quantified by
1019 qPCR using strain specific primers (Supplemental Table 5). For qPCR, genomic DNA from cell
1020 pellets of competition mixtures was extracted using either the Qiagen Blood & Tissue kit
1021 following the protocol for extraction from Gram-negative organisms or via mechanical lysis as
1022 described above. DNA was quantified via Qubit (ThermoFisher) and diluted before using as
1023 template DNA in qPCR (SsoAdvanced, BioRad). All experiments were performed with technical
1024 triplicates for at least three biological replicates.
1025
1026 **Gnotobiotic mouse colonization studies**
1027 *Animal care*
1028 In accordance with protocols approved by the University of Washington Institutional
1029 Animal Care and Use Committee, germ-free 5-12 week old male and female Swiss Webster mice
1030 from multiple litters were randomly selected and housed in pairs in single Techniplast cages with
1031 a 12-hour light/dark cycle and fed a standard lab diet (Laboratory Autoclavable Rodent Diet
1032 5010, LabDiet). Blinding was not performed. For each experiment, the number of animals per
1033 group (n=4) was selected based on Lemorte power calculations to measure a difference of ~10-
1034 fold bacterial abundance with a $p < 0.05$ at 80% power along with housing and maintenance
1035 considerations for gnotobiotic mice. Mouse feces were confirmed to be sterile prior to
1036 colonization by PCR with primers targeting the 16S rRNA gene.
1037

1038 *Mouse colonization procedures*

1039 Bacterial strains to be employed in germ-free mouse colonization experiments were
1040 grown anaerobically on Brucella-blood plates, resuspended in BHI broth, and diluted. For
1041 experiments to determine strain competitiveness in a simplified context, pairs of strains were
1042 combined at a 100:1 (10^9 :10^7 CFU, *B. acidifaciens: P. vulgatus*) or 10:1 ratio (10^9: 10^8 CFU, all
1043 other donor–recipient pairs), as determined by prior calculation of the OD600 to CFU
1044 correspondence. This mixture was introduced into germ-free mice via oral gavage (200 µL per
1045 mouse).

1046 To colonize mice with the WildR microbiome and a genetically modified WildR isolate
1047 (e.g., *B. acid* ^{exo}), we first estimated the approximate abundance of the endogenous isolate (e.g.,
1048 *B. acid* ^{endo}*)* in the WildR stocks using a combination of CFU enumeration, qPCR, and 16S
1049 rRNA sequencing. The total CFU of Bacteroidales strains from the *Bacteroides*, *Phocaeicola*,
1050 and *Parabacteroides* in the WildR reference stocks was determined by plating on Brucella-blood
1051 agar supplemented with gentamycin, a condition selective for the order. The abundance of *B.*
1052 *acidifaciens* relative to total Bacteroidales levels in WildR stocks was then determined using
1053 qPCR with species and order-specific primers on DNA extracted from WildR reference stocks,
1054 and this measurement was used to estimate the contribution of CFUs from *B. acidifaciens* to the
1055 total Bacteroidales population (~$3x10^4$ CFU/ml of WildR cryopreserved stocks). An estimate for
1056 the abundance of *P. vulgatus* CFUs in WildR stocks (~$3x10^6$ CFU/ml) was calculated in a
1057 similar manner, except the fraction of total Bacteroidales represented by this strain was
1058 determined by counting reads from 16S rRNA gene sequencing of amplicons from WildR
1059 reference stock genomic DNA, as described below.

1060 Modified strains to be introduced to mice along with the WildR community were grown
1061 and suspended in BHI broth as described above for isolate colonization studies. Suspensions
1062 were then diluted to the desired CFU level (~$3x10^4$, $3x10^5$ or $3x10^6$ *B. acid* ^{exo} CFU or ~$3x10^7$ *P.*
1063 *vul* ^{exo} CFU) in 1 mL of the WildR reference stock under anaerobic conditions. After preparation,
1064 the mixture was stored in Wheaton crimp top vials to maintain an anaerobic environment and
1065 then introduced into germ-free Swiss Webster mice via a single oral gavage (150-200 µL per
1066 mouse). For all germ-free mouse colonization experiments, levels of introduced strains in the
1067 gavage mixtures were determined by diluting and plating on selective media.
1068
1069 *Quantification of bacterial populations in fecal and cecal samples*
1070 Fresh fecal pellets were collected from colonized animals at regular intervals, and cecal
1071 contents were collected from euthanized animals at the conclusion of the experiment as
1072 described for WildR reference stock generation. To enumerate CFUs of marked strains, fresh
1073 fecal pellets or cecal contents (~50-100 mg/sample) were homogenized in PBS using sterile
1074 pestles. Insoluble material was removed via gentle centrifugation (500 x*g*, 30s) and the resulting
1075 supernatant was diluted in PBS. Dilutions were plated on selective media (e.g., Brucella-blood
1076 supplemented with erythromycin and gentamycin to isolate *B. acid* ^{exo} from the WildR
1077 community) and incubated anaerobically at 37 ˚C. Final CFU counts were normalized to initial
1078 fecal weights. Remaining fecal or cecal material from these collections was stored at -80 ˚C for
1079 gDNA extraction.
1080 The abundance of modified strains relative to total bacteria present or endogenous
1081 populations in WildR-colonized mice was determined by qPCR. Genomic DNA was extracted
1082 from thawed fecal pellets or cecal contents (~50-100 mg/sample) by first combining samples

1083 with 200 µL of 0.1-mm-diameter zirconia/silica beads (BioSpec Products, Bartlesville, OK), 500
1084 µL of CP Buffer (Omega Biotek, #PDR042) or PB Buffer (Qiagen), 250 µL of 20% SDS, and
1085 550 µL of phenol:chloroform:isoamyl alcohol (24:24:1) (ThermoFisher). Microbial cells were
1086 mechanically lysed with a bead beater at room temperature (BioSpec Products; instrument on
1087 high for 1 min; 2 cycles) and then centrifuged at 10,000 *xg* for 10 min to separate phases. All of
1088 the aqueous phase containing gDNA (~400-500 µL/sample) was applied to E-Z 96™ DNA
1089 plates (Omega Biotek; #BD96-01) or Qiagen Blood and Tissue columns and cleaned following
1090 the standard protocol. DNA was quantified by fluorimetry (Qubit, ThermoFisher) and then
1091 diluted to ~5 ng/uL in EB (10 mM Tris-HCl pH 8.5; Omega Biotek PDR048). Relative species
1092 or strain abundance was determined by qPCR using primers described in Supplemental Table 5.
1093 All qPCR was performed using a CFX96 instrument (BioRad) and SsoAdvanced Universal
1094 SYBR Green Supermix (BioRad).
1095
1096 *Community structure analysis by 16S rRNA gene amplicon*
1097 The V3-V4 region of the 16S rRNA gene was amplified from genomic DNA extracted
1098 from fecal and cecal samples following the standard Illumina protocol for 16S metagenomic
1099 sequencing (Illumina Part # 15044223 Rev. B) with the following modifications. Briefly,
1100 purified gDNA was quantified by Qubit, diluted to 5 ng/µL, and amplified using primers
1101 16S_v3v4_fwd_Illumina and 16S_v3v4_rev_Illumina (Supplemental Table 5) and 2x KAPA
1102 HiFi HotStart ReadyMix (Roche). PCR was performed in triplicate to avoid jackpot
1103 amplification. Reactions were prepared in a biosafety cabinet to prevent contamination and each
1104 run included no-template controls. Pooled PCR products for each sample were cleaned using
1105 AmpureXP beads (Bruker). A second PCR was performed to add sequencing adapters and

1106 barcodes (IDT for Illumina UD Indexes Plates A-D) using 2x KAPA HiFi HotStart ReadyMix.
1107 Final PCR products were cleaned and normalized with the Sequalprep Normalization Plate kit
1108 (Thermo Scientific). The size and quantity of DNA libraries from select samples was confirmed
1109 by agarose gel electrophoresis and fluorimetry (Qubit), respectively.

1110 Equal volumes of 16S rRNA libraries prepared from up to 384 samples was pooled and
1111 quantified for sequencing. Libraries were denatured, diluted, and combined with PhiX spike-in
1112 before sequencing on the MiSeq or NextSeq2000 (300-bp paired reads; dual 10 bp indexes; 10 or
1113 25% PhiX, respectively). Samples were demultiplexed with onboard software for each
1114 instrument. All data generated from this sequencing has been deposited with links to BioProject
1115 PRJNA1367654 in the NCBI database.

1116 Analysis of 16S rRNA sequencing data was performed using Qiime2 (v2020.11; (Bolyen
1117 et al. 2019)). Primers were trimmed using the qiime cutadapt plugin before using DADA2 for
1118 ASV calling and counting to determine the relative abundance of each ASV. Beta diversity
1119 metrics (Unifrac) were calculated from rarefied data using the qiime diversity plugin and
1120 statistical tests were performed with the qiime longitudinal plugin. Principle component analysis
1121 plots were generated in R using cmdscale. To quantify total *B. acidifaciens* abundance, we
1122 performed a custom taxonomic assignment of ASVs. The top taxonomic hit for each ASV was
1123 obtained by a BLAST search of each ASV in the WildR MAG and isolate genome catalog.
1124 These new taxonomic assignments were combined with relative abundance of each ASV
1125 calculated from the DADA2 analysis to determine relative frequencies of *B. acidifaciens*.
1126

1127 **ICE-seq library preparation and data analysis**

1128 Genomic DNA was extracted from fecal samples as described above and used to prepare
1129 ICE-seq libraries following previously described methods with the modifications described
1130 below (Gallagher 2019) (Supplemental Figure 4A). Briefly, DNA was sheared to ~500 bp
1131 average size and C-tailed. Sequences outside of the ICE at either the 5' or 3' ends of the ICE were
1132 specifically amplified using primers annealing within the ICE at either the 5' or 3' end ("ICE
1133 junction") and a C-tailed specific primer (Supplemental Table 5). After DNA purification, a
1134 second round of PCR was performed to amplify the ICE junctions and add adapter and index
1135 sequences for sequencing. Samples were pooled and multiplexed samples were sequenced as 75-
1136 bp single-end reads on an Illumina MiniSeq with 30% PhiX DNA spiked in using a custom mix
1137 containing three primers for sequencing the 5', 3', and PhiX sequences.
1138 Illumina sequencing reads were analyzed using a portion of previously described custom
1139 Python script (Gallagher 2019). Sequences were filtered for those containing the first 5 bp
1140 (ATAAT) or 7 bp (ATTATTG) of the ICE 5' and 3' ends, respectively. Then reads were aligned
1141 using a BWA aligner to a composite CMMG-WildR catalog, which was dereplicated (at 99%
1142 ANI) using dRep (v3.5.0) (Olm et al. 2017, Kieser et al. 2022). Reads per insertion site were
1143 tallied, and insertion sites were filtered to include only sites where reads mapped in opposite
1144 directions from both ends of the ICE. To calculate the percentage of ICE reads mapping in a
1145 sample, the total of mapped reads fitting these criteria was calculated and the fraction of each
1146 insertion site was then determined. The percentage was independently calculated for reads
1147 generated from either end of the ICE. Sequencing reads have been deposited with links to
1148 BioProject PRJNA1367654 in the NCBI database.
1149
1150 **Statistical analysis**

1151 Statistical analysis was performed using GraphPad Prism (version 10.2.3 for Mac OS X,

1152 GraphPad Software, Boston, Massachusetts USA, www.graphpad.com) using tests described in

1153 the main text and figure legends.

1154

1155

1156 **References**

1157 Alneberg, J., B. S. Bjarnason, I. de Bruijn, M. Schirmer, J. Quick, U. Z. Ijaz, L. Lahti, N. J.
1158 Loman, A. F. Andersson and C. Quince (2014). "Binning metagenomic contigs by coverage and
1159 composition." Nat Methods **11**(11): 1144-1146.

1160 Altschul, S. F., W. Gish, W. Miller, E. W. Myers and D. J. Lipman (1990). "Basic local
1161 alignment search tool." Journal of molecular biology **215**(3): 403–410.

1162 Bacic, M. K. and C. J. Smith (2008). "Laboratory maintenance and cultivation of bacteroides
1163 species." Curr Protoc Microbiol **Chapter 13**: Unit 13C 11.

1164 Bencivenga-Barry, N. A., B. Lim, C. M. Herrera, M. S. Trent and A. L. Goodman (2020).
1165 "Genetic Manipulation of Wild Human Gut Bacteroides." J Bacteriol **202**(3).

1166 Bolger, A. M., M. Lohse and B. Usadel (2014). "Trimmomatic: a flexible trimmer for Illumina
1167 sequence data." Bioinformatics **30**(15): 2114-2120.

1168 Bolyen, E., J. R. Rideout, M. R. Dillon, N. A. Bokulich, C. C. Abnet, G. A. Al-Ghalith, H.
1169 Alexander, E. J. Alm, M. Arumugam, F. Asnicar, Y. Bai, J. E. Bisanz, K. Bittinger, A. Brejnrod,
1170 C. J. Brislawn, C. T. Brown, B. J. Callahan, A. M. Caraballo-Rodriguez, J. Chase, E. K. Cope, R.
1171 Da Silva, C. Diener, P. C. Dorrestein, G. M. Douglas, D. M. Durall, C. Duvallet, C. F.
1172 Edwardson, M. Ernst, M. Estaki, J. Fouquier, J. M. Gauglitz, S. M. Gibbons, D. L. Gibson, A.
1173 Gonzalez, K. Gorlick, J. Guo, B. Hillmann, S. Holmes, H. Holste, C. Huttenhower, G. A.
1174 Huttley, S. Janssen, A. K. Jarmusch, L. Jiang, B. D. Kaehler, K. B. Kang, C. R. Keefe, P. Keim,
1175 S. T. Kelley, D. Knights, I. Koester, T. Kosciolek, J. Kreps, M. G. I. Langille, J. Lee, R. Ley, Y.
1176 X. Liu, E. Loftfield, C. Lozupone, M. Maher, C. Marotz, B. D. Martin, D. McDonald, L. J.
1177 McIver, A. V. Melnik, J. L. Metcalf, S. C. Morgan, J. T. Morton, A. T. Naimey, J. A. Navas-
1178 Molina, L. F. Nothias, S. B. Orchanian, T. Pearson, S. L. Peoples, D. Petras, M. L. Preuss, E.
1179 Pruesse, L. B. Rasmussen, A. Rivers, M. S. Robeson, 2nd, P. Rosenthal, N. Segata, M. Shaffer,
1180 A. Shiffer, R. Sinha, S. J. Song, J. R. Spear, A. D. Swafford, L. R. Thompson, P. J. Torres, P.
1181 Trinh, A. Tripathi, P. J. Turnbaugh, S. Ul-Hasan, J. J. J. van der Hooft, F. Vargas, Y. Vazquez-
1182 Baeza, E. Vogtmann, M. von Hippel, W. Walters, Y. Wan, M. Wang, J. Warren, K. C. Weber, C.
1183 H. D. Williamson, A. D. Willis, Z. Z. Xu, J. R. Zaneveld, Y. Zhang, Q. Zhu, R. Knight and J. G.
1184 Caporaso (2019). "Reproducible, interactive, scalable and extensible microbiome data science
1185 using QIIME 2." Nat Biotechnol **37**(8): 852-857.

1186 Chatzidaki-Livanis, M., N. Geva-Zatorsky and L. E. Comstock (2016). "Bacteroides fragilis type
1187 VI secretion systems use novel effector and immunity proteins to antagonize human gut
1188 Bacteroidales species." Proc Natl Acad Sci U S A **113**(13): 3627–3632.

1189 Chaumeil, P. A., A. J. Mussig, P. Hugenholtz and D. H. Parks (2019). "GTDB-Tk: a toolkit to
1190 classify genomes with the Genome Taxonomy Database." Bioinformatics **36**(6): 1925-1927.

1191 Coulthurst, S. (2019). "The Type VI secretion system: a versatile bacterial weapon."
1192 Microbiology **165**(5): 503–515.

1193 Coyne, M. J., K. G. Roelofs and L. E. Comstock (2016). "Type VI secretion systems of human
1194 gut Bacteroidales segregate into three genetic architectures, two of which are contained on
1195 mobile genetic elements." BMC Genomics **17**: 58.

1196 Coyne, M. J., N. L. Zitomersky, A. M. McGuire, A. M. Earl and L. E. Comstock (2014).
1197 "Evidence of Extensive DNA Transfer between Bacteroidales Species within the Human Gut."
1198 mBio **5**(3).

1199 Coyte, K. Z. and S. Rakoff-Nahoum (2019). "Understanding Competition and Cooperation
1200 within the Mammalian Gut Microbiome." Curr Biol **29**(11): R538-R544.

1201 Coyte, K. Z., J. Schluter and K. R. Foster (2015). "The ecology of the microbiome: Networks,
1202 competition, and stability." Science **350**(6261): 663–666.

1203 Deatherage, D. E. and J. E. Barrick (2014). "Identification of mutations in laboratory-evolved
1204 microbes from next-generation sequencing data using breseq." Methods Mol Biol **1151**: 165-188.

1205 Dimitriu, T., M. D. Szczelkun and E. R. Westra (2024). "Various plasmid strategies limit the
1206 effect of bacterial restriction-modification systems against conjugation." Nucleic Acids Res
1207 **52**(21): 12976-12986.

1208 Duran, D., P. Bernal, D. Vazquez-Arias, E. Blanco-Romero, D. Garrido-Sanz, M. Redondo-
1209 Nieto, R. Rivilla and M. Martin (2021). "Pseudomonas fluorescens F113 type VI secretion
1210 systems mediate bacterial killing and adaption to the rhizosphere microbiome." Sci Rep **11**(1):
1211 5772.

1212 Gallagher, L. A. (2019). "Methods for Tn-Seq Analysis in Acinetobacter baumannii." Methods
1213 Mol Biol **1946**: 115-134.

1214 Garcia-Bayona, L. and L. E. Comstock (2018). "Bacterial antagonism in host-associated
1215 microbial communities." Science **361**(6408).

1216 Garcia-Bayona, L. and L. E. Comstock (2019). "Streamlined Genetic Manipulation of Diverse
1217 Bacteroides and Parabacteroides Isolates from the Human Gut Microbiota." mBio **10**(4).

1218 Garcia-Bayona, L., M. J. Coyne and L. E. Comstock (2021). "Mobile Type VI secretion system
1219 loci of the gut Bacteroidales display extensive intra-ecosystem transfer, multi-species spread and
1220 geographical clustering." PLoS Genet **17**(4): e1009541.

1221 Hecht, A. L., B. W. Casterline, Z. M. Earley, Y. A. Goo, D. R. Goodlett and J. Bubeck
1222 Wardenburg (2016). "Strain competition restricts colonization of an enteric pathogen and
1223 prevents colitis." EMBO Rep **17**(9): 1281–1291.

1224 Hill, C. A., B. W. Casterline, E. Valguarnera, A. L. Hecht, E. S. Shepherd, J. L. Sonnenburg and
1225 J. Bubeck Wardenburg (2024). "Bacteroides fragilis toxin expression enables lamina propria
1226 niche acquisition in the developing mouse gut." Nat Microbiol **9**(1): 85-94.

1227 Hood, R. D., P. Singh, F. Hsu, T. Guvener, M. A. Carl, R. R. Trinidad, J. M. Silverman, B. B.
1228 Ohlson, K. G. Hicks, R. L. Plemel, M. Li, S. Schwarz, W. Y. Wang, A. J. Merz, D. R. Goodlett
1229 and J. D. Mougous (2010). "A type VI secretion system of Pseudomonas aeruginosa targets a
1230 toxin to bacteria." Cell Host Microbe **7**(1): 25–37.

1231 Javdan, B., J. G. Lopez, P. Chankhamjon, Y. J. Lee, R. Hull, Q. Wu, X. Wang, S. Chatterjee and
1232 M. S. Donia (2020). "Personalized Mapping of Drug Metabolism by the Human Gut
1233 Microbiome." Cell **181**(7): 1661-1679 e1622.

1234 Jin, W. B., T. T. Li, D. Huo, S. Qu, X. V. Li, M. Arifuzzaman, S. F. Lima, H. Q. Shi, A. Wang,
1235 G. G. Putzel, R. S. Longman, D. Artis and C. J. Guo (2022). "Genetic manipulation of gut
1236 microbes enables single-gene interrogation in a complex microbiome." Cell **185**(3): 547-562
1237 e522.

1238 Johnston, C. D., S. L. Cotton, S. R. Rittling, J. R. Starr, G. G. Borisy, F. E. Dewhirst and K. P.
1239 Lemon (2019). "Systematic evasion of the restriction-modification barrier in bacteria." Proc Natl
1240 Acad Sci U S A **116**(23): 11454-11459.

1241 Kang, D. D., F. Li, E. Kirton, A. Thomas, R. Egan, H. An and Z. Wang (2019). "MetaBAT 2: an
1242 adaptive binning algorithm for robust and efficient genome reconstruction from metagenome
1243 assemblies." PeerJ **7**: e7359.

1244 Kieser, S., E. M. Zdobnov and M. Trajkovski (2022). "Comprehensive mouse microbiota
1245 genome catalog reveals major difference to its human counterpart." PLoS Comput Biol **18**(3):
1246 e1009947.

1247 Kolmogorov, M., J. Yuan, Y. Lin and P. A. Pevzner (2019). "Assembly of long, error-prone
1248 reads using repeat graphs." Nat Biotechnol **37**(5): 540-546.

1249 Koropatkin, N. M., E. C. Martens, J. I. Gordon and T. J. Smith (2008). "Starch catabolism by a
1250 prominent human gut symbiont is directed by the recognition of amylose helices." Structure
1251 **16**(7): 1105–1115.

1252 Langmead, B. and S. L. Salzberg (2012). "Fast gapped-read alignment with Bowtie 2." Nat
1253 Methods **9**(4): 357–359.

1254 Lee, S. M., G. P. Donaldson, Z. Mikulski, S. Boyajian, K. Ley and S. K. Mazmanian (2013).
1255 "Bacterial colonization factors control specificity and stability of the gut microbiota." Nature
1256 **501**(7467): 426–429.

1257 Li, H. (2018). "Minimap2: pairwise alignment for nucleotide sequences." Bioinformatics **34**(18):
1258 3094-3100.

1259 Li, H., B. Handsaker, A. Wysoker, T. Fennell, J. Ruan, N. Homer, G. Marth, G. Abecasis, R.
1260 Durbin and S. Genome Project Data Processing (2009). "The Sequence Alignment/Map format
1261 and SAMtools." Bioinformatics **25**(16): 2078-2079.

1262 Lu, J., F. P. Breitwieser, P. Thielen and S. L. Salzberg (2017). "Bracken: estimating species
1263 abundance in metagenomics data." PeerJ Comput Sci **3**.

1264 Maghini, D. G., E. L. Moss, S. E. Vance and A. S. Bhatt (2021). "Improved high-molecular-
1265 weight DNA extraction, nanopore sequencing and metagenomic assembly from the human gut
1266 microbiome." Nat Protoc **16**(1): 458-471.

1267 Maldonado-Gomez, M. X., I. Martinez, F. Bottacini, A. O'Callaghan, M. Ventura, D. van
1268 Sinderen, B. Hillmann, P. Vangay, D. Knights, R. W. Hutkins and J. Walter (2016). "Stable
1269 Engraftment of Bifidobacterium longum AH1206 in the Human Gut Depends on Individualized
1270 Features of the Resident Microbiome." Cell Host Microbe **20**(4): 515-526.

1271 Marchler-Bauer, A., J. B. Anderson, F. Chitsaz, M. K. Derbyshire, C. DeWeese-Scott, J. H.
1272 Fong, L. Y. Geer, R. C. Geer, N. R. Gonzales, M. Gwadz, S. He, D. I. Hurwitz, J. D. Jackson, Z.
1273 Ke, C. J. Lanczycki, C. A. Liebert, C. Liu, F. Lu, S. Lu, G. H. Marchler, M. Mullokandov, J. S.
1274 Song, A. Tasneem, N. Thanki, R. A. Yamashita, D. Zhang, N. Zhang and S. H. Bryant (2009).
1275 "CDD: specific functional annotation with the Conserved Domain Database." Nucleic Acids Res
1276 **37**(Database issue): D205–210.

1277 Martinez, I., M. X. Maldonado-Gomez, J. C. Gomes-Neto, H. Kittana, H. Ding, R. Schmaltz, P.
1278 Joglekar, R. J. Cardona, N. L. Marsteller, S. W. Kembel, A. K. Benson, D. A. Peterson, A. E.
1279 Ramer-Tait and J. Walter (2018). "Experimental evaluation of the importance of colonization
1280 history in early-life gut microbiota assembly." Elife **7**.

1281 Motta, E. V. S., P. J. Lariviere, K. R. Jones, Y. Song and N. A. Moran (2024). "Type VI
1282 secretion systems promote intraspecific competition and host interactions in a bee gut symbiont."
1283 Proc Natl Acad Sci U S A **121**(44): e2414882121.

1284 Obadia, B., Z. T. Guvener, V. Zhang, J. A. Ceja-Navarro, E. L. Brodie, W. W. Ja and W. B.
1285 Ludington (2017). "Probabilistic Invasion Underlies Natural Gut Microbiome Stability." Curr
1286 Biol **27**(13): 1999-2006 e1998.

1287 Olm, M. R., C. T. Brown, B. Brooks and J. F. Banfield (2017). "dRep: a tool for fast and
1288 accurate genomic comparisons that enables improved genome recovery from metagenomes
1289 through de-replication." ISME J **11**(12): 2864-2868.

1290 Parks, D. H., M. Imelfort, C. T. Skennerton, P. Hugenholtz and G. W. Tyson (2015). "CheckM:
1291 assessing the quality of microbial genomes recovered from isolates, single cells, and
1292 metagenomes." Genome Res **25**(7): 1043-1055.

1293 Robitaille, S., E. L. Simmons, A. J. Verster, E. A. McClure, D. B. Royce, E. Trus, K. Swartz, D.
1294 Schultz, C. D. Nadell and B. D. Ross (2023). "Community composition and the environment
1295 modulate the population dynamics of type VI secretion in human gut bacteria." Nat Ecol Evol
1296 **7**(12): 2092-2107.

1297 Ross, B. D., A. J. Verster, M. C. Radey, D. T. Schmidtke, C. E. Pope, L. R. Hoffman, A. M.
1298 Hajjar, S. B. Peterson, E. Borenstein and J. D. Mougous (2019). "Human gut bacteria contain
1299 acquired interbacterial defence systems." Nature **575**(7781): 224–228.

1300 Rosshart, S. P., B. G. Vassallo, D. Angeletti, D. S. Hutchinson, A. P. Morgan, K. Takeda, H. D.
1301 Hickman, J. A. McCulloch, J. H. Badger, N. J. Ajami, G. Trinchieri, F. Pardo-Manuel de
1302 Villena, J. W. Yewdell and B. Rehermann (2017). "Wild Mouse Gut Microbiota Promotes Host
1303 Fitness and Improves Disease Resistance." Cell **171**(5): 1015-1028 e1013.

1304 Rubin, B. E., S. Diamond, B. F. Cress, A. Crits-Christoph, Y. C. Lou, A. L. Borges, H. Shivram,
1305 C. He, M. Xu, Z. Zhou, S. J. Smith, R. Rovinsky, D. C. J. Smock, K. Tang, T. K. Owens, N.
1306 Krishnappa, R. Sachdeva, R. Barrangou, A. M. Deutschbauer, J. F. Banfield and J. A. Doudna
1307 (2022). "Species- and site-specific genome editing in complex bacterial communities." Nat
1308 Microbiol **7**(1): 34-47.

1309 Russell, A. B., A. G. Wexler, B. N. Harding, J. C. Whitney, A. J. Bohn, Y. A. Goo, B. Q. Tran,
1310 N. A. Barry, H. Zheng, S. B. Peterson, S. Chou, T. Gonen, D. R. Goodlett, A. L. Goodman and J.
1311 D. Mougous (2014). "A type VI secretion-related pathway in Bacteroidetes mediates
1312 interbacterial antagonism." Cell Host Microbe **16**(2): 227–236.

1313 Salipante, S. J., D. J. Sengupta, L. A. Cummings, A. Robinson, K. Kurosawa, D. R. Hoogestraat
1314 and B. T. Cookson (2014). "Whole genome sequencing indicates Corynebacterium jeikeium
1315 comprises 4 separate genomospecies and identifies a dominant genomospecies among clinical
1316 isolates." Int J Med Microbiol **304**(8): 1001-1010.

1317 Schwarz, S., T. E. West, F. Boyer, W. C. Chiang, M. A. Carl, R. D. Hood, L. Rohmer, T. Tolker-
1318 Nielsen, S. J. Skerrett and J. D. Mougous (2010). "Burkholderia type VI secretion systems have
1319 distinct roles in eukaryotic and bacterial cell interactions." PLoS Pathog **6**(8): e1001068.

1320 Seemann, T. (2014). "Prokka: rapid prokaryotic genome annotation." Bioinformatics **30**(14):
1321 2068-2069.

1322 Segura Munoz, R. R., S. Mantz, I. Martinez, F. Li, R. J. Schmaltz, N. A. Pudlo, K. Urs, E. C.
1323 Martens, J. Walter and A. E. Ramer-Tait (2022). "Experimental evaluation of ecological
1324 principles to understand and modulate the outcome of bacterial strain competition in gut
1325 microbiomes." ISME J **16**(6): 1594-1604.

1326 Sheahan, M. L., K. Flores, M. J. Coyne, L. Garcia-Bayona, M. Chatzidaki-Livanis, A. Q. Holst,
1327 R. C. Smith, A. Sundararajan, B. Barquera and L. E. Comstock (2024). "A ubiquitous mobile
1328 genetic element changes the antagonistic weaponry of a human gut symbiont." Science
1329 **386**(6720): 414-420.

1330 Smith, C. J., M. B. Rogers and M. L. McKee (1992). "Heterologous gene expression in
1331 Bacteroides fragilis." Plasmid **27**(2): 141-154.

1332 Speare, L., A. G. Cecere, K. R. Guckes, S. Smith, M. S. Wollenberg, M. J. Mandel, T. Miyashiro
1333 and A. N. Septer (2018). "Bacterial symbionts use a type VI secretion system to eliminate
1334 competitors in their natural host." Proc Natl Acad Sci **115**(36): E8528–E8537.

1335 Uritskiy, G. V., J. DiRuggiero and J. Taylor (2018). "MetaWRAP-a flexible pipeline for
1336 genome-resolved metagenomic data analysis." Microbiome **6**(1): 158.

1337 Van Damme, R., M. Holzer, A. Viehweger, B. Muller, E. Bongcam-Rudloff and C. Brandt
1338 (2021). "Metagenomics workflow for hybrid assembly, differential coverage binning,
1339 metatranscriptomics and pathway analysis (MUFFIN)." PLoS Comput Biol **17**(2): e1008716.

1340 van Kempen, M., S. S. Kim, C. Tumescheit, M. Mirdita, J. Lee, C. L. M. Gilchrist, J. Soding and
1341 M. Steinegger (2023). "Fast and accurate protein structure search with Foldseek." Nat
1342 Biotechnol.

1343 Vazquez-Arias, D., C. Civantos, D. Duran-Wendt, A. Ruiz, R. Rivilla, M. Martin and P. Bernal
1344 (2025). "The Pseudomonas putida type VI secretion systems shape the tomato rhizosphere
1345 microbiota." ISME Commun **5**(1): ycaf158.

1346 Verster, A. J., B. D. Ross, M. C. Radey, Y. Bao, A. L. Goodman, J. D. Mougous and E.
1347 Borenstein (2017). "The Landscape of Type VI Secretion across Human Gut Microbiomes
1348 Reveals Its Role in Community Composition." Cell Host Microbe **22**(3): 411–419 e414.

1349 Walker, B. J., T. Abeel, T. Shea, M. Priest, A. Abouelliel, S. Sakthikumar, C. A. Cuomo, Q.
1350 Zeng, J. Wortman, S. K. Young and A. M. Earl (2014). "Pilon: an integrated tool for
1351 comprehensive microbial variant detection and genome assembly improvement." PLoS One
1352 **9**(11): e112963.

1353 Wang, J., N. B. Shoemaker, G. R. Wang and A. A. Salyers (2000). "Characterization of a
1354 Bacteroides mobilizable transposon, NBU2, which carries a functional lincomycin resistance
1355 gene." J Bacteriol **182**(12): 3559-3571.

1356 Wexler, A. G., Y. Bao, J. C. Whitney, L. M. Bobay, J. B. Xavier, W. B. Schofield, N. A. Barry,
1357 A. B. Russell, B. Q. Tran, Y. A. Goo, D. R. Goodlett, H. Ochman, J. D. Mougous and A. L.
1358 Goodman (2016). "Human symbionts inject and neutralize antibacterial toxins to persist in the
1359 gut." Proc Natl Acad Sci **113**(13): 3639–3644.

1360 Whitaker, W. R., E. S. Shepherd and J. L. Sonnenburg (2017). "Tunable Expression Tools
1361 Enable Single-Cell Strain Distinction in the Gut Microbiome." Cell **169**(3): 538-546 e512.

1362 Whitney, J. C., S. B. Peterson, J. Kim, M. Pazos, A. J. Verster, M. C. Radey, H. D. Kulasekara,
1363 M. Q. Ching, N. P. Bullen, D. Bryant, Y. A. Goo, M. G. Surette, E. Borenstein, W. Vollmer and
1364 J. D. Mougous (2017). "A broadly distributed toxin family mediates contact-dependent
1365 antagonism between gram-positive bacteria." Elife **6**(Jul 11): e26938.

1366 Wick, R. R. and K. E. Holt (2019). "Benchmarking of long-read assemblers for prokaryote
1367 whole genome sequencing." F1000Res **8**: 2138.

1368 Wick, R. R. and K. E. Holt (2022). "Polypolish: Short-read polishing of long-read bacterial
1369 genome assemblies." PLoS Comput Biol **18**(1): e1009802.

1370 Wick, R. R., L. M. Judd, L. T. Cerdeira, J. Hawkey, G. Meric, B. Vezina, K. L. Wyres and K. E.
1371 Holt (2021). "Trycycler: consensus long-read assemblies for bacterial genomes." Genome Biol
1372 **22**(1): 266.

1373 Wick, R. R., L. M. Judd, C. L. Gorrie and K. E. Holt (2017). "Unicycler: Resolving bacterial
1374 genome assemblies from short and long sequencing reads." PLoS Comput Biol **13**(6): e1005595.

1375 Wood, D. E., J. Lu and B. Langmead (2019). "Improved metagenomic analysis with Kraken 2."
1376 Genome Biol **20**(1): 257.

1377 Zhang, Z. J., C. G. Cole, M. J. Coyne, H. Lin, N. Dylla, R. C. Smith, T. E. Pappas, S. A.
1378 Townson, N. Laliwala, E. Waligurski, R. Ramaswamy, C. Woodson, V. Burgo, J. C. Little, D.
1379 Moran, A. Rose, M. McMillin, E. McSpadden, A. Sundararajan, A. M. Sidebottom, E. G. Pamer
1380 and L. E. Comstock (2024). "Comprehensive analyses of a large human gut Bacteroidales culture
1381 collection reveal species- and strain-level diversity and evolution." Cell Host Microbe **32**(10):
1382 1853-1867 e1855.
1383

Figure 1

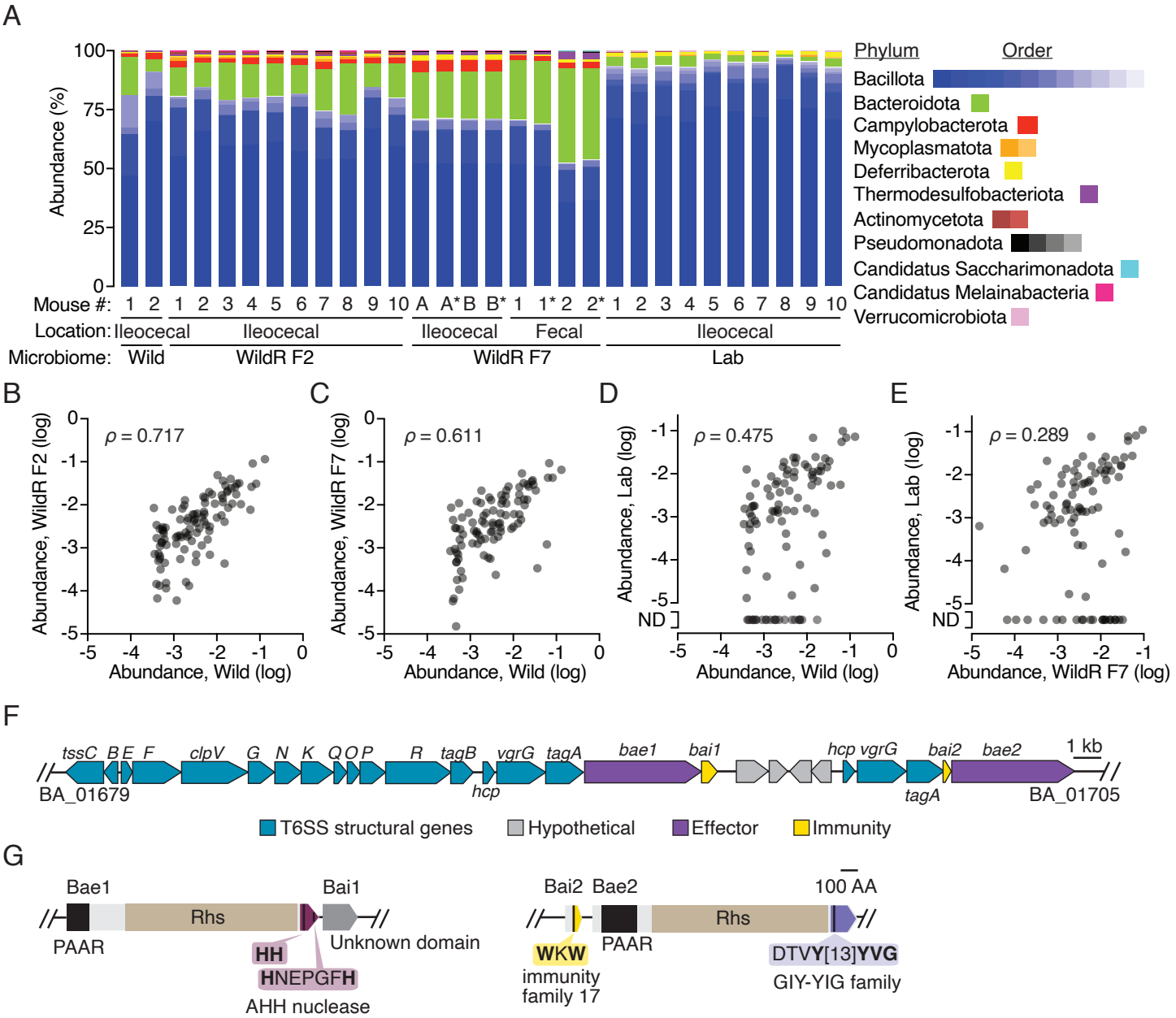
A
Abundance (%)
Mouse #: 1 2 1 2 3 4 5 6 7 8 9 10 A A*B B* 1 1* 2 2* 1 2 3 4 5 6 7 8 9 10
Location: Ileocecal Ileocecal Ileocecal Fecal Ileocecal
Microbiome: Wild WildR F2 WildR F7 Lab
Phylum Order
Bacillota
Bacteroidota
Campylobacterota
Mycoplasmatota
Deferribacterota
Thermodesulfobacteriota
Actinomycetota
Pseudomonadota
Candidatus Saccharimonadota
Candidatus Melainabacteria
Verrucomicrobiota
B
ρ = 0.717
Abundance, WildR F2 (log)
Abundance, Wild (log)
C
ρ = 0.611
Abundance, WildR F7 (log)
Abundance, Wild (log)
D
ρ = 0.475
Abundance, Lab (log)
ND
Abundance, Wild (log)
E
ρ = 0.289
Abundance, Lab (log)
ND
Abundance, WildR F7 (log)
F
tssC B E F clpV G N K Q O P R tagB vgrG tagA bae1 bai1 hcp vgrG bai2 bae2
1 kb
BA_01679
hcp
tagA
BA_01705
T6SS structural genes
Hypothetical
Effector
Immunity
G
Bae1
Rhs
Bai1
PAAR
HH
HNEPGFH
Unknown domain
AHH nuclease
Bai2 Bae2
100 AA
Rhs
WKW
PAAR
immunity family 17
DTVY[13]YVG
GIY-YIG family

Figure 2

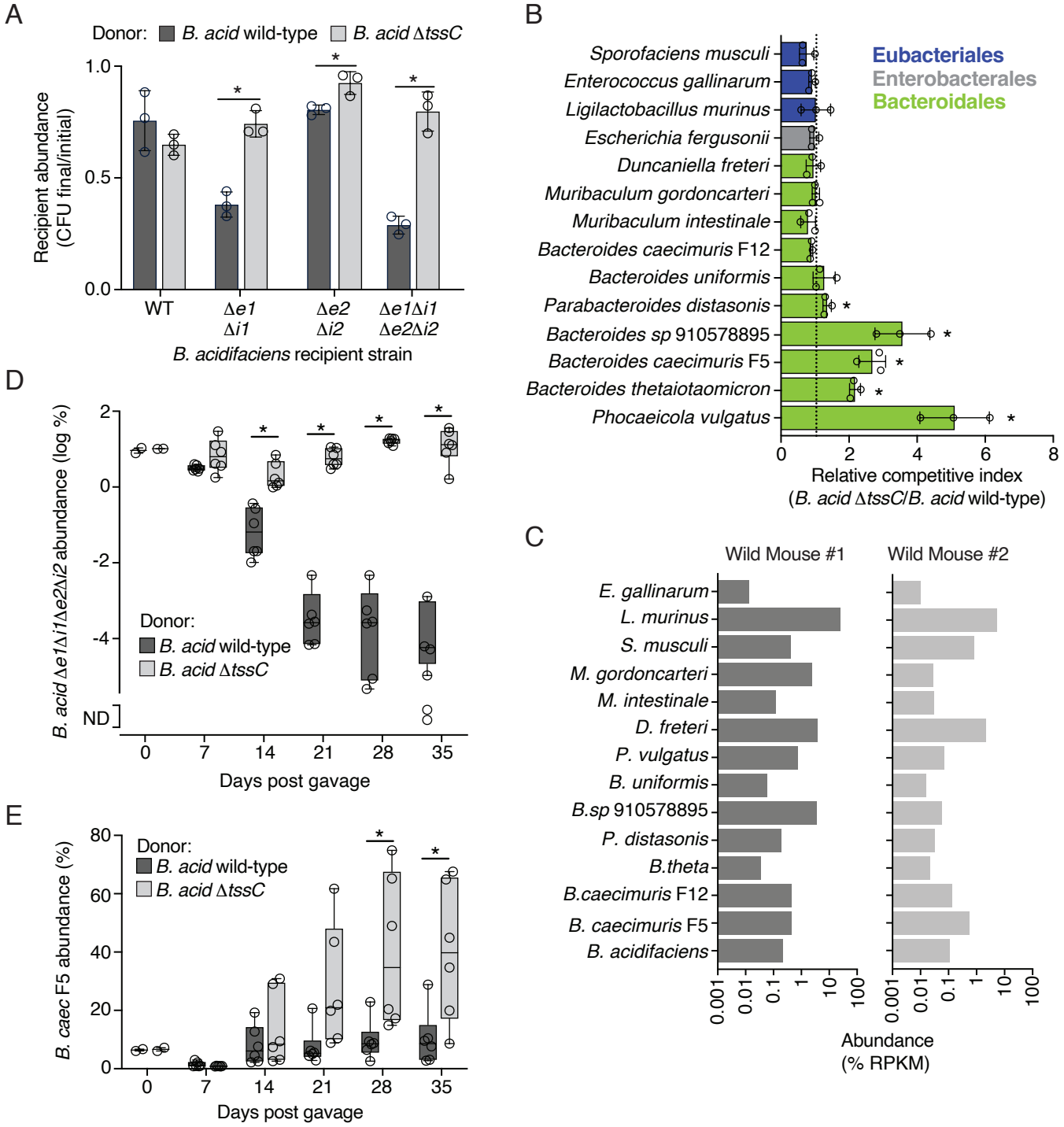
A
Donor: B. acid wild-type B. acid ΔtssC
Recipient abundance (CFU final/initial)
1.0
0.5
0.0
WT
Δe1 Δi1
Δe2 Δi2
Δe1Δi1 Δe2Δi2
B. acidifaciens recipient strain
B
Sporofaciens musculi
Enterococcus gallinarum
Ligilactobacillus murinus
Escherichia fergusonii
Duncaniella freteri
Muribaculum gordoncarteri
Muribaculum intestinale
Bacteroides caecimuris F12
Bacteroides uniformis
Parabacteroides distasonis
Bacteroides sp 910578895
Bacteroides caecimuris F5
Bacteroides thetaiotaomicron
Phocaeicola vulgatus
Eubacteriales
Enterobacterales
Bacteroidales
0 2 4 6 8
Relative competitive index
(B. acid ΔtssC/B. acid wild-type)
D
B. acid Δe1Δi1Δe2Δi2 abundance (log %)
2
0
-2
-4
ND
Donor:
B. acid wild-type
B. acid ΔtssC
0 7 14 21 28 35
Days post gavage
C
Wild Mouse #1
Wild Mouse #2
E. gallinarum
L. murinus
S. musculi
M. gordoncarteri
M. intestinale
D. freteri
P. vulgatus
B. uniformis
B.sp 910578895
P. distasonis
B.theta
B.caecimuris F12
B. caecimuris F5
B. acidifaciens
0.001 0.01 0.1 1 10 100
Abundance
(% RPKM)
E
B. caec F5 abundance (%)
80
60
40
20
0
Donor:
B. acid wild-type
B. acid ΔtssC
0 7 14 21 28 35
Days post gavage

Figure 3

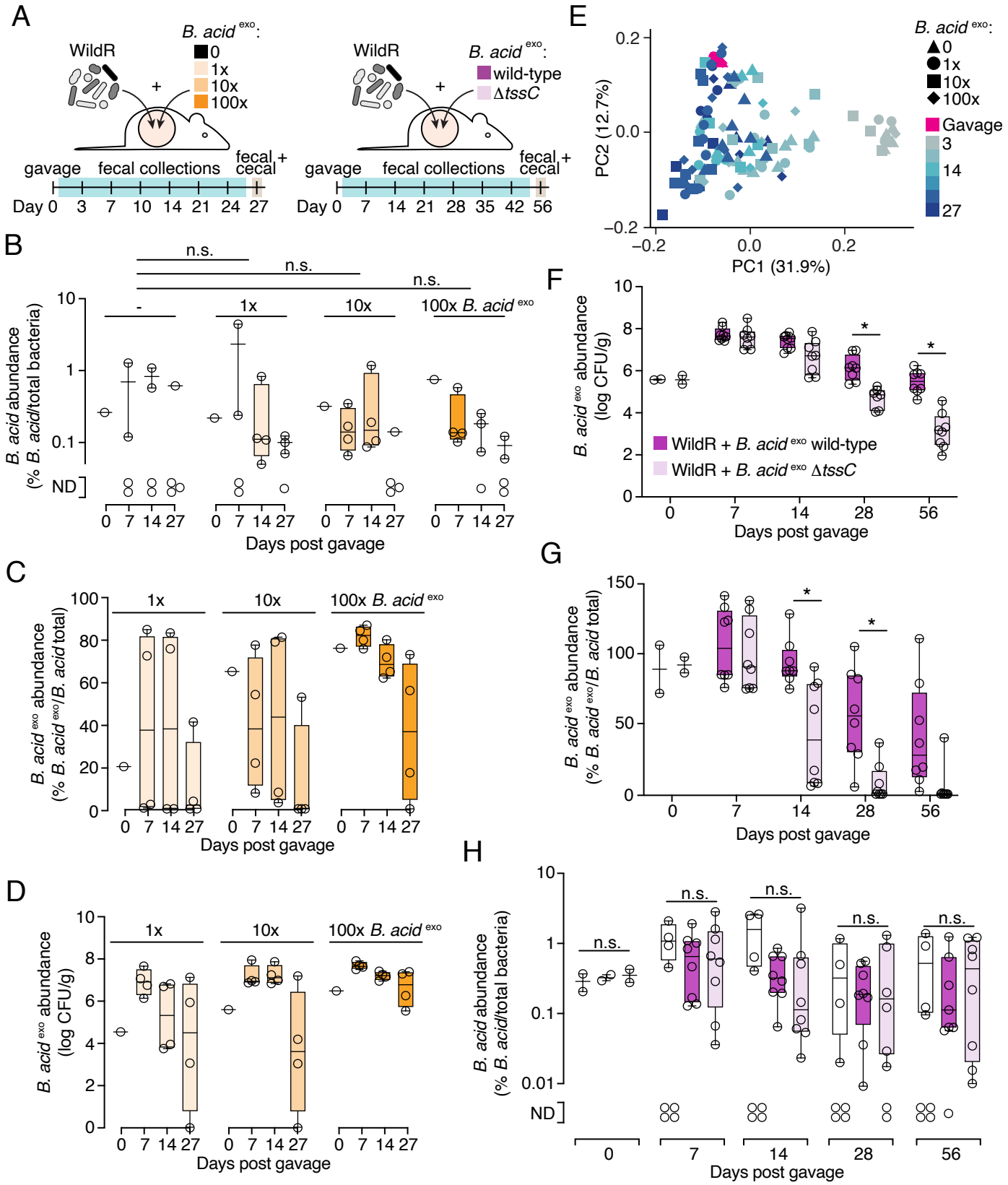
A
WildR
B. acid exo:
0
1x
10x
100x
gavage
fecal collections
fecal + cecal
Day 0 3 7 10 14 21 24 27
WildR
B. acid exo:
wild-type
ΔtssC
gavage
fecal collections
fecal + cecal
Day 0 7 14 21 28 35 42 56
B
n.s.
n.s.
n.s.
-
1x
10x
100x B. acid exo
B. acid abundance (% B. acid/total bacteria)
ND
Days post gavage
C
1x
10x
100x B. acid exo
B. acid exo abundance (% B. acid exo/B. acid total)
Days post gavage
D
1x
10x
100x B. acid exo
B. acid exo abundance (log CFU/g)
Days post gavage
E
B. acid exo:
0
1x
10x
100x
Gavage
3
14
27
PC2 (12.7%)
PC1 (31.9%)
F
B. acid exo abundance (log CFU/g)
WildR + B. acid exo wild-type
WildR + B. acid exo ΔtssC
Days post gavage
G
B. acid exo abundance (% B. acid exo/B. acid total)
Days post gavage
H
n.s.
B. acid abundance (% B. acid/total bacteria)
ND
Days post gavage

Figure 4

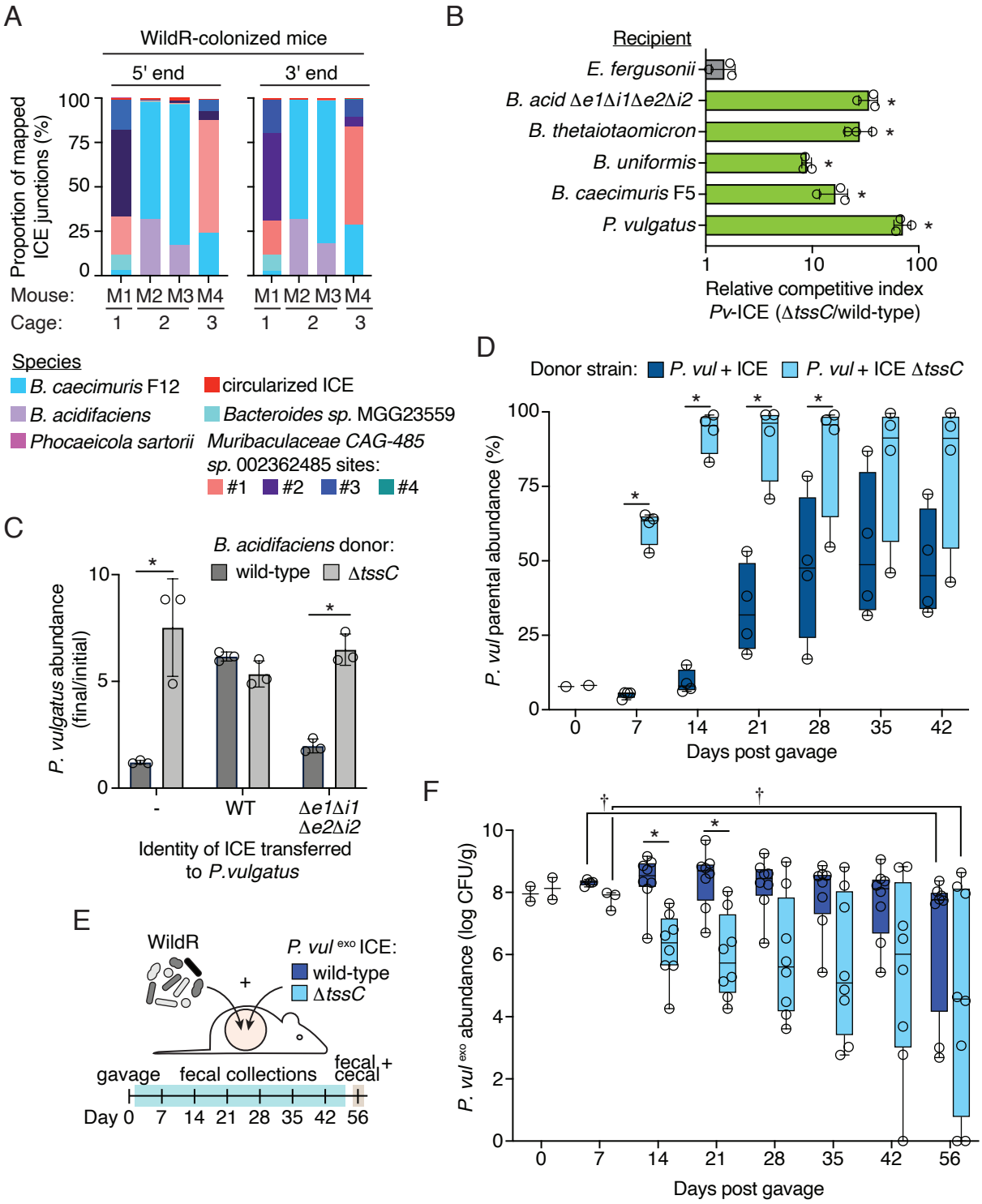
A
WildR-colonized mice
5' end
3' end
Proportion of mapped ICE junctions (%)
100
75
50
25
0
Mouse:
M1 M2 M3 M4
M1 M2 M3 M4
Cage:
1 2 3
1 2 3
Species
B. caecimuris F12
circularized ICE
B. acidifaciens
Bacteroides sp. MGG23559
Phocaeicola sartorii
Muribaculaceae CAG-485 sp. 002362485 sites:
#1 #2 #3 #4
B
Recipient
E. fergusonii
B. acid Δe1Δi1Δe2Δi2
B. thetaiotaomicron
B. uniformis
B. caecimuris F5
P. vulgatus
1
10
100
Relative competitive index
Pv-ICE (ΔtssC/wild-type)
C
B. acidifaciens donor:
wild-type
ΔtssC
P. vulgatus abundance (final/initial)
10
5
0
-
WT
Δe1Δi1 Δe2Δi2
Identity of ICE transferred to P.vulgatus
D
Donor strain: P. vul + ICE
P. vul + ICE ΔtssC
P. vul parental abundance (%)
100
75
50
25
0
0 7 14 21 28 35 42
Days post gavage
E
WildR
P. vul exo ICE:
wild-type
ΔtssC
+
gavage
fecal collections
fecal + cecal
Day 0 7 14 21 28 35 42 56
F
P. vul exo abundance (log CFU/g)
10
8
6
4
2
0
0 7 14 21 28 35 42 56
Days post gavage

Supplemental Figure 1

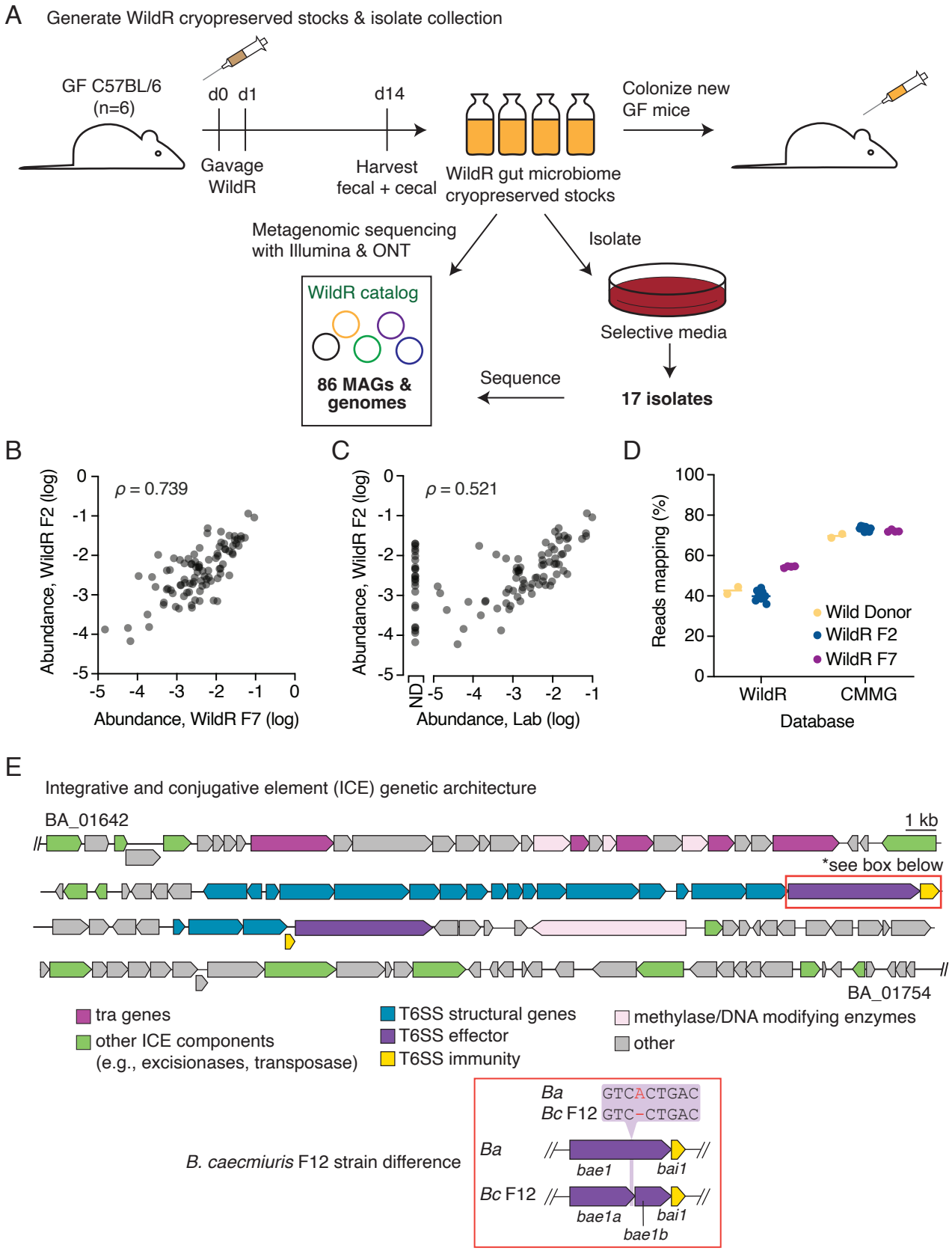

Supplemental Figure 2

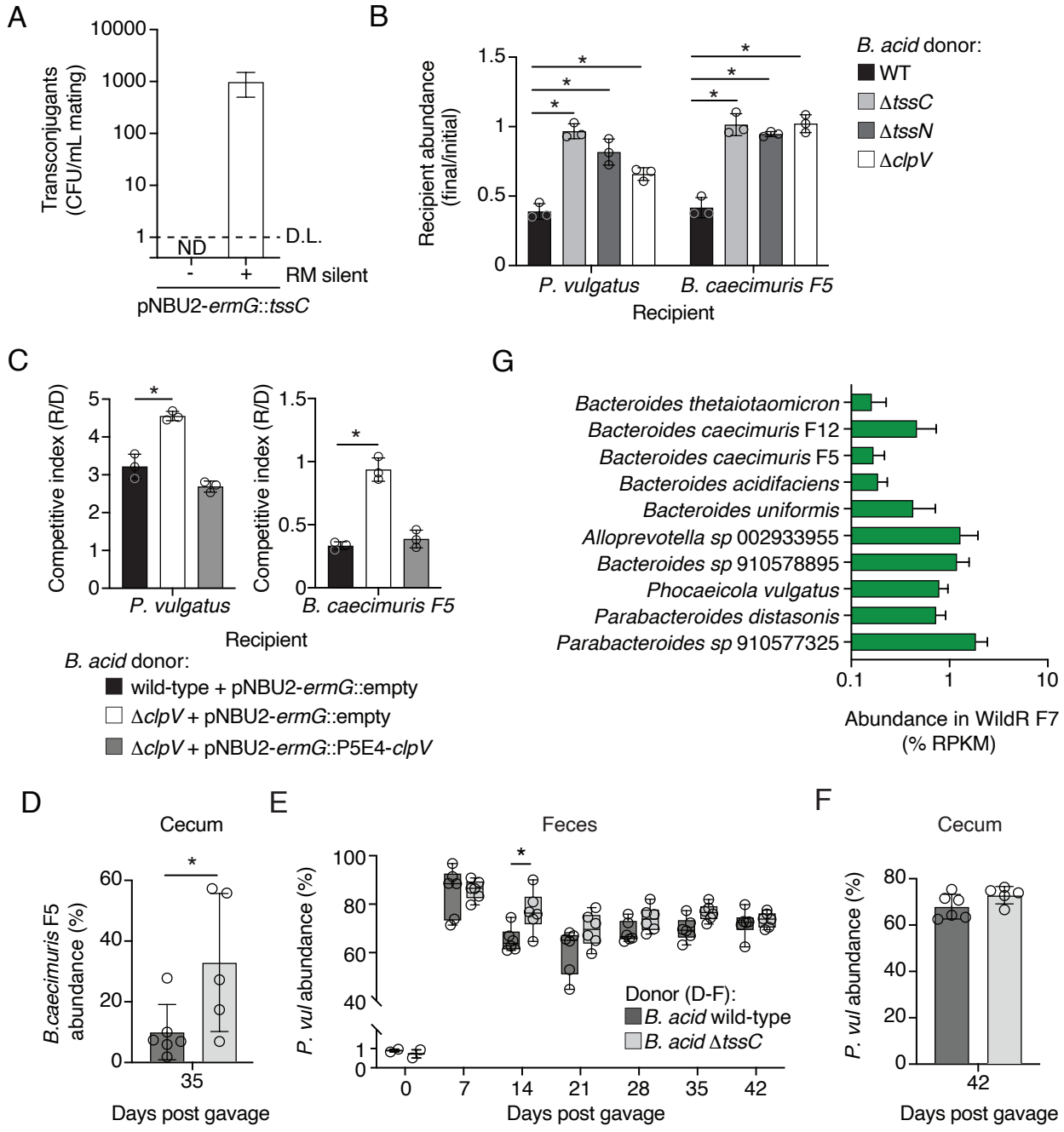

Supplemental Figure 3

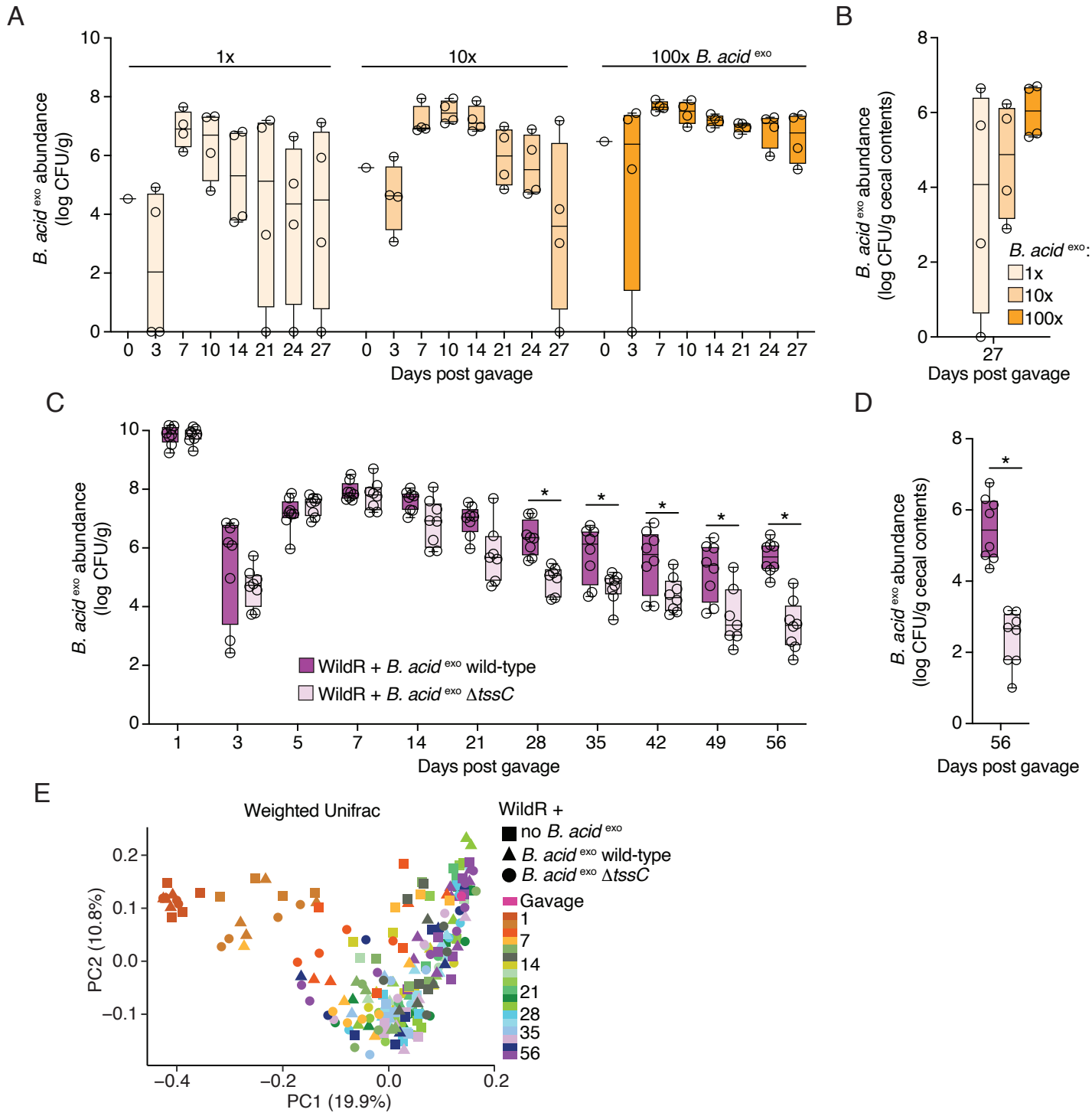
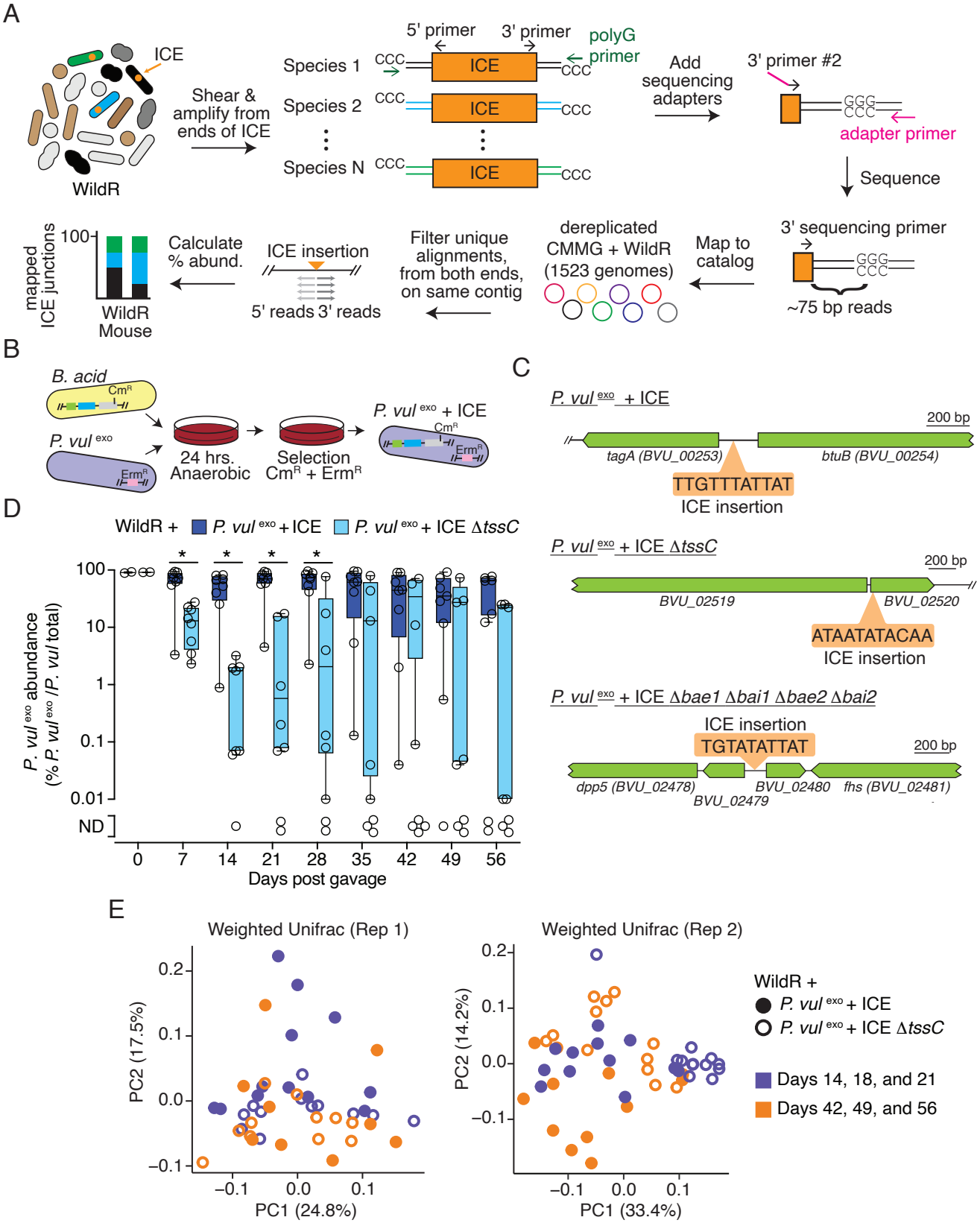
Supplemental Figure 4